

UNCLASSIFIED

AD NUMBER

ADB017021

LIMITATION CHANGES

TO:

Approved for public release; distribution is unlimited.

FROM:

Distribution authorized to U.S. Gov't. agencies only; Test and Evaluation; NOV 1976. Other requests shall be referred to Rome Air Development Center, Griffiss AFB, NY.

AUTHORITY

RADC ltr 18 Apr 1977

THIS PAGE IS UNCLASSIFIED

THIS REPORT HAS BEEN DELIMITED
AND CLEARED FOR PUBLIC RELEASE
UNDER DOD DIRECTIVE 5200.20 AND
NO RESTRICTIONS ARE IMPOSED UPON
ITS USE AND DISCLOSURE.

DISTRIBUTION STATEMENT A

APPROVED FOR PUBLIC RELEASE;
DISTRIBUTION UNLIMITED.

RADC-TR-76-269(I)

IN-HOUSE REPORT

NOVEMBER 1976



ADBO17021

Computer Solutions to Heat and Diffraction Equations in High Energy Laser Windows

Volume I

PETER D. GIANINO
BERNARD BENDOW
N. GRIER PARKE, III
THEODORE B. BARRETT



Distribution limited to U.S. Government Agencies only
(Test & Evaluation); (November 1976). Other requests
for this document must be referred to RADC-ETE,
Hanscom AFB, Massachusetts 01731


AD NO. —
DDC FILE COPY

ROME AIR DEVELOPMENT CENTER
AIR FORCE SYSTEMS COMMAND
GRIFFISS AIR FORCE BASE, NEW YORK 13441


APPROVAL SHEET

This technical report has been reviewed and approved by RADC (OI) for publication.

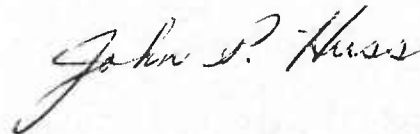
APPROVED:


NICHOLAS F. YANNONI, Chief
Optical Techniques Branch
Solid State Sciences Division

APPROVED:


ROBERT M. BARRETT
Director
Solid State Sciences Division

FOR THE COMMANDER:



Unclassified

SECURITY CLASSIFICATION OF THIS PAGE (When Data Entered)

| REPORT DOCUMENTATION PAGE | | READ INSTRUCTIONS BEFORE COMPLETING FORM |
|---|-----------------------|---|
| 1. REPORT NUMBER RADC-TR-76-269 ⑩ -Vol-1 | 2. GOVT ACCESSION NO. | 3. RECIPIENT'S CATALOG NUMBER |
| 4. TITLE (and Subtitle) COMPUTER SOLUTIONS TO HEAT AND DIFFRACTION EQUATIONS IN HIGH ENERGY LASER WINDOWS Volume I | | 5. TYPE OF REPORT & PERIOD COVERED Scientific. Interim. |
| 6. AUTHOR(s) Peter D. Gianino, N. Grier/Parke, III* Bernard Bendow, Theodore B. Barrett* | | 7. PERFORMING ORG. REPORT NUMBER |
| 8. PERFORMING ORGANIZATION NAME AND ADDRESS Deputy for Electronic Technology (RADC/ETSS) Hanscom AFB Massachusetts 01731 | | 9. CONTRACT OR GRANT NUMBER(s) |
| 10. CONTROLLING OFFICE NAME AND ADDRESS Deputy for Electronic Technology (RADC/ETSS) Hanscom AFB Massachusetts 01731 | | 11. PROGRAM ELEMENT, PROJECT, TASK AND WORK UNIT NUMBERS 62601F 33260802 |
| 12. MONITORING AGENCY NAME & ADDRESS (if different from Controlling Office) ⑨ Interim rept. | | 13. REPORT DATE 11 November 1976 |
| 14. DISTRIBUTION STATEMENT (of this Report) Distribution limited to U. S. Government Agencies only; (Test & Evaluation); (November 1976). Other requests for this document must be referred to RADC/ETE, Hanscom AFB, Massachusetts 01731 | | 15. NUMBER OF PAGES 50 |
| 16. DISTRIBUTION STATEMENT (of the abstract entered in Block 20, if different from Report) ① 3326 ① 17081 | | 17. SECURITY CLASS. (of this report) Unclassified |
| 18. DECLASSIFICATION/DOWNGRADING SCHEDULE | | |
| 19. SUPPLEMENTARY NOTES * Parke Mathematical Laboratories, Inc. Carlisle, Mass. 01741 | | |
| 20. KEY WORDS (Continue on reverse side if necessary and identify by block number) Laser windows Numerical solution of heat equation Laser window materials Thermal lensing Numerical solution of vector Kirchhoff diffraction equation | | |
| 21. ABSTRACT (Continue on reverse side if necessary and identify by block number) The LQ-10 Infrared Laser Window Program was initiated at AFCRL (now RADC/DET) in 1971 to develop a mechanically superior, highly trans- mitting optical window for CO ₂ and chemical lasers to be used by the Air Force for military applications. From the earliest stages of that program it became evident that the principal failure mechanism of the window would be thermal lensing, that is, the distorting and defocusing of the laser beam as it propagated through the solid. For this reason analytical tools were | | |

DD FORM 1 JAN 73 1473 EDITION OF 1 NOV 65 IS OBSOLETE

Unclassified

SECURITY CLASSIFICATION OF THIS PAGE (When Data Entered)

* laser

309 050

Unclassified

SECURITY CLASSIFICATION OF THIS PAGE(When Data Entered)

20. Abstract (Continued)

developed to predict the extent of this lensing in various candidate materials under a variety of conditions. This work contributed to selection of appropriate materials, as well as to design of geometrical configurations, in which the lensing could be reduced. To quantify the effects of thermal lensing, an efficient computer program package was developed and programmed to run on a CDC6600 computer. The package was written to handle Gaussian-shaped beams incident on either a thin disc- or annular-shaped cylindrical window. Three coupled programs make up the package: TEMP5, which solves the full heat transport equation within the window for any given set of initial and boundary conditions on each surface; TIKIRK, which solves the vector Kirchhoff diffraction integrals for the beam transmitted to the far field; and DISPLAY, which plots these temperatures and/or intensities in a variety of ways, including three-dimensional perspective views. Volume I of this report lays the theoretical foundations underlying these programs and presents graphical results for two model problems using disc- and annular-shaped windows. Volume II is a "user's manual." It describes how each program functions, enumerates the constituent subroutines and subprograms, gives complete Fortran listings, and even provides typical detailed commands to initiate and run the programs in both the Intercom and Batch modes of operation. Results of this work should substantially aid engineers in planning configurations and specifications for current and conceptual systems.

| | |
|---------------------------------|-------------------------------------|
| White Section | <input type="checkbox"/> |
| Blue Section | <input checked="" type="checkbox"/> |
| Red Section | <input type="checkbox"/> |
| UNCLASSIFIED | |
| JUSTIFICATION | |
| BY | |
| DISTRIBUTION/AVAILABILITY CODES | |
| Dist. | ATL. and/or SPECIAL |
| B | |

Unclassified

SECURITY CLASSIFICATION OF THIS PAGE(When Data Entered)

Contents

VOLUME I

| | |
|--|----|
| 1. INTRODUCTION | 9 |
| 2. PLAN | 11 |
| 3. THE HEAT PROBLEM | 11 |
| 3.1 The Heat Equation | 11 |
| 3.2 The Heat Source Term | 13 |
| 3.3 The Boundary Condition Equation | 15 |
| 4. THE FAR-FIELD INTENSITY PATTERN | 17 |
| 5. THE PROGRAMMED FORMS OF THE HEAT AND BC EQUATIONS | 21 |
| 5.1 Nondimensional Form | 21 |
| 5.2 A Dimensioned Form | 22 |
| 6. GRAPHS FOR TWO MODEL PROBLEMS | 24 |
| 6.1 Description of the Models | 24 |
| 6.2 Multiple X-Y Plots | 24 |
| 6.2.1 X-Y Temperature Plots | 24 |
| 6.2.2 X-Y Intensity Plots | 25 |
| 6.3 Perspective Plots | 36 |
| 6.3.1 Perspective Temperature Plots | 36 |
| 6.3.2 Perspective Intensity Plots | 40 |
| 6.4 Contour Plots | 43 |
| REFERENCES | 49 |

Contents

VOLUME II

| | |
|---|-----|
| 7. INTRODUCTION | 59 |
| 8. TEMP5 PROGRAM | 60 |
| 8.1 Introductory Remarks | 60 |
| 8.2 Finite Difference Analogs for the General BC's | 61 |
| 8.3 Finite Difference Equations for I.A.D. Method | 63 |
| 8.4 The Solution of a Tridiagonal System of Equations | 65 |
| 8.5 Putting the I.A.D. Equations into Tridiagonal Form | 68 |
| 8.6 The Time Coordinate | 71 |
| 8.7 The Main Program and Principal Subroutines | 73 |
| 8.8 Implementation of Some of the Subroutines | 74 |
| 8.8.1 DATINIT | 75 |
| 8.8.2 CYLTMP | 75 |
| 8.8.3 TRIDAG | 75 |
| 8.8.4 GETDATA | 75 |
| 8.8.4.1 Description | 75 |
| 8.8.4.2 List Mode | 91 |
| 8.8.4.3 Name-Value Mode | 92 |
| 8.8.4.4 Entry-Parameter List | 93 |
| 8.8.4.5 Algorithm | 94 |
| 8.8.4.6 Special Caution and Features | 94 |
| 9. TIKIRK PROGRAM | 96 |
| 9.1 Introductory Remarks | 96 |
| 9.2 Program Options | 96 |
| 9.3 Principal Functions and Subroutines | 96 |
| 9.4 Inputting the Data | 98 |
| 9.5 Program Files | 98 |
| 9.6 Implementing the Program | 101 |
| 9.6.1 General Instructions | 101 |
| 9.6.2 Special Instructions for IKIRKP Option | 102 |
| 9.7 The IKIRK1 Option and an Alternate TIKIRK Package | 103 |
| 10. DISPLAY PROGRAM | 105 |
| 10.1 Introductory Remarks | 105 |
| 10.2 General Instructions | 106 |
| 10.3 Data Cards | 107 |
| 10.4 Command Cards | 109 |
| 10.5 Examples of the Use of the Three Different Plotting Commands | 111 |
| 10.6 Principal Functions and Subroutines | 114 |
| 10.7 Algorithms | 115 |
| 10.7.1 Multiple X-Y Displays | 115 |
| 10.7.2 Perspective Display | 115 |
| 10.7.3 Contour Display | 116 |
| 10.8 Batch and Intercom Modes | 116 |
| 10.9 Other Features | 117 |
| 10.10 Program Files | 117 |
| 11. OTHER CAPABILITIES | 118 |
| REFERENCES | 121 |

Contents

| | |
|---|-----|
| ATTACHMENT 1. Commands to Run TEMP5 and TIKIRK | 123 |
| ATTACHMENT 2. Commands to Modify a Temperature Distribution | 129 |
| ATTACHMENT 3. Commands to Recalculate TIKIRK, Given TEMP5 Results | 133 |
| ATTACHMENT 4. Commands to Produce a TAPE8 for Temperature Plots | 135 |
| ATTACHMENT 5. Commands for Running Alternate TIKIRK Program | 139 |
| ATTACHMENT 6. Batch Commands for Running DISPLAY Program | 143 |
| APPENDIX A. Fortran Listings for TEMP5 Program | 147 |
| APPENDIX B. Fortran Listings for TIKIRK Program, Options No. 1 and No. 2, Only | 165 |
| APPENDIX C. The Evaluation of $I^1(u, o, t)$ and $I^1(o, v, t)$ Used in the IKIRKP Option | 189 |
| APPENDIX D. Fortran Listings for the Main Programs in the Alternate TIKIRK Package Containing All Three Options | 195 |
| APPENDIX E. Fortran Listings for DISPLAY Program | 211 |
| APPENDIX F. Fortran Listing for Program T3D | 241 |

Illustrations

VOLUME I

| | |
|--|----|
| 1. Normalized Window Coordinates | 13 |
| 2. Cylindrical Coordinates for the Field Point in Space | 19 |
| 3. Temperature Versus Axial Distance in the Window at Zero Radial Position at the 9 Times Indicated, Using Model No. 1 | 26 |
| 4. Same as Figure 3, but at a Radial Distance of 15 cm | 27 |
| 5. Same as Figure 3, but at a Radial Distance of 30 cm, that is, Just Inside the Outer Edge | 28 |
| 6. Temperature Versus Axial Distance in the Window for 3 Different Radial Positions at $t = 5$ sec, Using Model No. 1 | 29 |
| 7A. Temperature Versus Radial Distance in the Window for 21 Different Axial Positions at Times of 1 Sec | 30 |
| 7B. Temperature Versus Radial Distance in the Window for 21 Different Axial Positions at Times of 5 Sec | 31 |

Illustrations

| | | |
|------|---|----|
| 8. | Temperature Versus Radial Distance in the Window in a Plane Through the Axis Which is Located 0.338 cm to the Left of the Window's Center at the 9 Times Indicated | 32 |
| 9. | Same as Figure 8, Except That the Plane is Located 0.307 cm to the Right of the Window's Center | 33 |
| 10. | Temperature Versus Radial Distance in the Window in an Axial Plane Approximately Through the Window's Center at the 9 Times Indicated | 34 |
| 11. | Same as Figure 10, Except That the Plane is Located Just Inside the Window's Exit Face | 35 |
| 12. | Laser Beam Intensity in the Far Field Versus Axial Distance Along the Axial Coordinate Itself (Zero Radial Distance) at the 9 Times Indicated, Using Model No. 1 | 37 |
| 13. | Laser Beam Intensity in the Far Field Versus Radial Distance in a Plane Perpendicular to the Axial Coordinate and at a Distance of 800 m Along the Axis for the 9 Times Indicated | 38 |
| 14. | Same as Figure 13, Except That it is in the Gaussian Focal Plane at Time $t = 3$ | 39 |
| 15. | Perspective Temperature Plot for Model No. 1 | 41 |
| 16. | Perspective Intensity Plots for Model No. 1 | 42 |
| 17A. | Contour Temperature Plots for Model No. 1 Showing 20 Temperature Contours at 2 Sec | 44 |
| 17B. | Contour Temperature Plots for Model No. 1 Showing 20 Temperature Contours at 8 Sec | 45 |
| 18A. | Contour Intensity Plots for Model No. 1 Showing 20 Intensity Contours at 2 Sec. | 46 |
| 18B. | Contour Intensity Plots for Model No. 1 Showing 20 Intensity Contours at 8 Sec | 47 |

VOLUME II

| | | |
|-----|-------------------------------------|----|
| 19. | Geometry of Finite Difference Net | 62 |
| 20. | Flow Chart for the CYLTMP Algorithm | 87 |

Tables

VOLUME I

| | | |
|----|--|----|
| 1. | Information on All the Parameters ($g_i, h_i, F_i, T_a, T_{s_i}$) for the Boundary Condition (BC) Equation | 17 |
|----|--|----|

Tables

VOLUME II

| | |
|--|-----|
| 2. Input Data for the Implementation of the TEMP5 Program | 76 |
| 3. Glossary of Variable Names | 82 |
| 4. Program Control Data and Constants Pertaining to the Calculation of the Intensity Function. | 99 |
| 5. Values Used for Certain TIKIRK Input Parameters Whenever IKIRKP is Employed | 103 |

Computer Solutions to Heat and Diffraction Equations in High Energy Laser Windows Volume I

1. INTRODUCTION

When a nonuniform high power laser beam traverses a nearly transparent material medium, the small amount of energy which is absorbed by the solid is often sufficient to raise its temperature by an appreciable amount. Since this heating is also nonuniform, it creates thermal stresses throughout the window which causes distortion and defocusing in the transmitted light beam; this phenomenon is called thermal lensing. This degradation of beam energy has been recognized as one of the principal failure modes in high-power laser windows.¹

In order to assess thermal lensing in an analytical manner, one must first determine how the temperature is varying throughout the medium as a function of time. This information must then be incorporated into a formalism which characterizes an optical beam traversing a material medium experiencing stress birefringence effects. From this, it now becomes possible to calculate how the

Received for publication 26 November 1976

1. Sparks, M. (1971) J. Appl. Phys. 42:5029; and, Jasperse, J. R., and Gianino, P. D. (1972) J. Appl. Phys. 43:1686.

transmitted beam will vary with time in the vicinity of the distant Gaussian focal point.²⁻⁷

To quantify the effects of thermal lensing, an efficient computer program package has been developed at AFCRL and programmed to run on a CDC6600 computer. The package has been written to handle an unpolarized, symmetric, Gaussian-shaped beam, incident uniaxially on either a thin disc -- or annular-shaped cylindrical window, which is assumed to be homogeneous and perfectly antireflective coated. Three coupled programs make up the package. One, called TEMP5, solves the full heat transport equation within the window for any given set of initial and boundary conditions on each surface. Its output is fed into the second program, called TIKIRK, which computes the intensity, or diffraction, pattern of the transmitted beam in the far field. The third program, called DISPLAY, has the capability of plotting the temperature and the intensity results from the first two programs in a variety of ways.

The TEMP5 heat program solves the partial differential heat equation by utilizing a numerical integration technique called the Implicit Alternating-Difference (I.A.D.) method, in which all finite difference analogs of all derivatives are correct to second order. The method employs a half increment shifted net because this allows the use of general boundary conditions. Being a fairly comprehensive program, it allows rather general specifications of the initial conditions, as well as different boundary conditions of the linear type on each surface. It is most accurate when a large number of spatial and temporal points are employed in the computation. The method is stable for all time increments which may be changed under program control. Various parameters pertaining to the beam shape and window geometry must be specified as input, along with the material's thermal and optical parameters and its boundary and initial conditions. The program computes the nondimensional temperature rise at each grid point in the window as a function of nondimensional time, as well as two aberration functions used by program TIKIRK.

All of these results, along with the remaining material and configurational parameters of the system, are then fed into the TIKIRK optical program. Here, specially designed integration routines compute the Hankel transforms and similar oscillatory-type integrals which evolve from the vector Kirchhoff diffraction theory.

2. Bendow, B., Jasperse, J.R., and Gianino, P.D. (1972) Optics Commun. 5:98.
3. Bendow, B., and Gianino, P.D. (1972) AFCRL-72-0322, unpublished.
4. Bendow, B., and Gianino, P.D. (1973) J. of Electronic Mater. 2:87.
5. Bendow, B., and Gianino, P.D. (1973) Appl. Optics 12:710.
6. Bendow, B., and Gianino, P.D. (1973) Appl. Phys. 2:1.
7. Gianino, P.D., and Bendow, B. (1973) Appl. Phys. 2:71.

The output gives the time behavior of the transmitted laser beam's intensity in the far field.

Program DISPLAY is a general purpose program which may be used to plot any function of two variables in any one or all of three ways — contour map, perspective view and multiple x-y plot. Since the temperature in the window and the intensity in the far field can be regarded as being functions of two space variables (as will shortly be shown), these lend themselves quite readily to plotting by this program. The third variable, time, is then considered to be a parameter, as far as the two-dimensional displays are concerned. As mentioned above, this program has the very desirable capability of a perspective plot. In this case, a surface representing temperature or intensity as a function of the two space variables can be drawn, giving the appearance of being a three-dimensional plot.

2. PLAN

We have divided this report into two parts. Our objective in Volume I is to give a brief introduction to the problem and to present the heat and diffraction equations appropriate to the geometric, physical, boundary and initial conditions imposed upon the problem. In this portion, we also define all of the parameters associated with the beam and the window and describe the four common types of boundary conditions expected to occur in the problem. Finally, we present in graphical form the results of a model problem in which a typical laser beam is incident on both a disc- and annular-shaped ZnSe window. These graphs show various two- and three-dimensional plots of both temperature in the window and intensity of the transmitted beam in space.

Volume II is a "user's manual." It describes the three computer programs in detail, explaining how they function and how they are implemented. It enumerates their constituent subroutines and subprograms, explains their functions and gives Fortran listings in appendices. In addition, attachments are provided which give typical detailed commands to initiate and run the programs in both the Intercom and Batch modes of operation.

3. THE HEAT PROBLEM

3.1 The Heat Equation

Since the incident beam and, therefore, the temperature distribution in the window have circular-cylindrical symmetry (there being no dependence on the angular coordinate θ), it will be sufficient to work with the two spatial coordinates

only, viz, r and z . The evaluation of the temperature at any point in this window requires the solution of the heat conduction equation, with the source term added, employing the boundary conditions at each surface and taking into account the initial temperature distribution through the window's interior. The heat conduction equation in the r, z cylindrical coordinates is given as:

$$\partial T / \partial t = \kappa \nabla_{r, z}^2 T + Q / c_p d \quad , \quad (1)$$

where

| | | |
|-------------------|---|------------------------|
| T | = temperature | [°C] |
| t | = time | [sec] |
| r | = radial coordinate | [cm] |
| z | = axial coordinate | [cm] |
| d | = density | [gm/cm ³] |
| c_p | = specific heat at constant pressure | [J/gm-°C] |
| κ | = thermal diffusivity $\equiv K / c_p d$ | [cm ² /sec] |
| K | = thermal conductivity | [W/cm-°C] |
| Q | = volume heating source | [W/cm ³] |
| $\nabla_{r, z}^2$ | $\equiv r^{-1} \partial / \partial r (r \partial / \partial r) + \partial^2 / \partial z^2$ | [cm ⁻²] |

The window has an axial thickness L and an outer radius a . When it is annular-shaped, the inner radius is designated by r_1 . However, rather than work with the coordinates and quantities as defined above, we will find it more convenient to deal with their dimensionless counterparts by normalizing to the outer radius " a ". These normalized terms are:

$$\begin{aligned} \rho &= r/a = \text{radial coordinate } (0 \leq \rho \leq 1) \\ \xi &= z/a = \text{axial coordinate} \\ \rho_1 &= r_1/a = \text{inner radius} \\ \rho_{12} &= (a - r_1)/a = \text{radial thickness} \\ \xi_{12} &= L/a = \text{axial thickness} \end{aligned}$$

We choose the ρ, ξ coordinate system such that its origin is at the center of the sample. The window face through which the laser beam enters is located at $\xi_1 (\equiv -L/2a)$. The laser beam travels in the positive ξ direction and exits at the face given by $\xi_2 (\equiv L/2a)$. This coordinate system and the geometrical quantities defined above are depicted superimposed on the window in Figure 1.

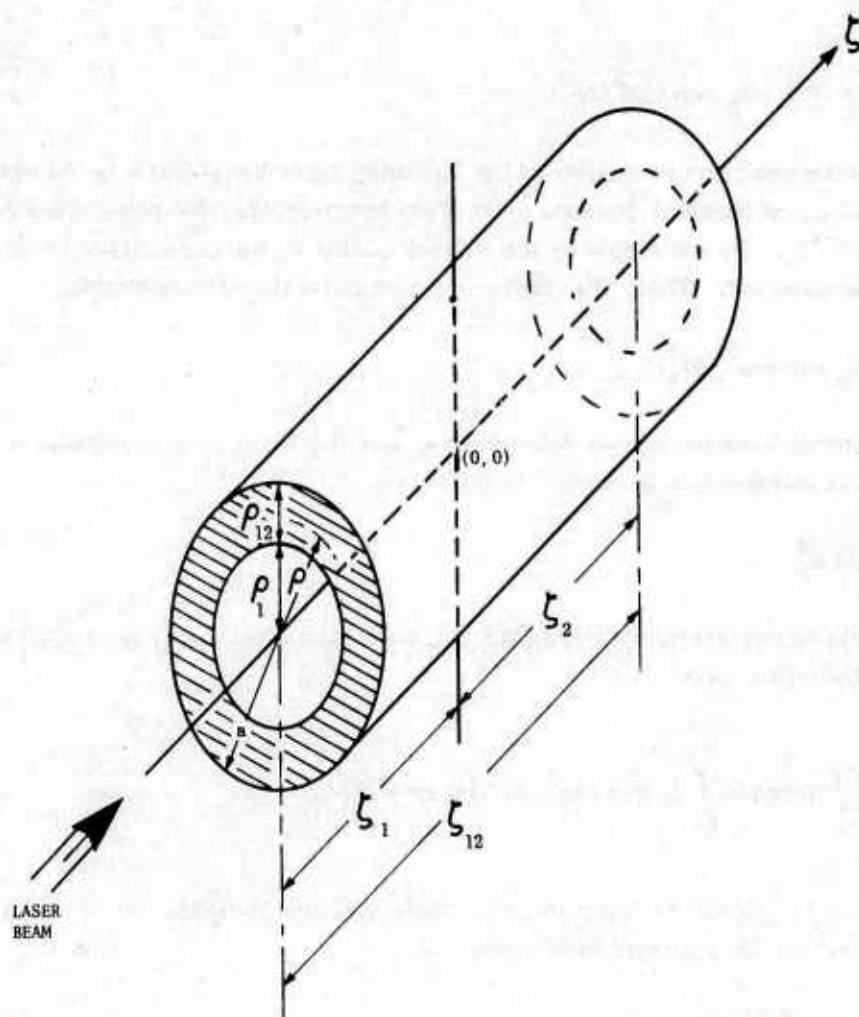


Figure 1. Normalized Window Coordinates. "a" is the outer radius (in cm)

3.2 The Heat Source Term

In general, the source term Q may be a function of r and z (but not of time, except that it may be "turned off" at a particular time). However, it is most convenient to assume that it is given as the product of the bulk absorption coefficient β and the laser beam power density $I(r, z)$ at that point. Typically, I has dimensions of W/cm^2 and β in cm^{-1} . The power density function is separable in the r, z coordinates, that is, $I(r, z) = I(r)I(z)$. Under the usual assumption that β is sufficiently small so that β times thickness $\ll 1$ always, then $I(z) \approx 1$. It is also assumed that the incident laser beam is Gaussian-shaped and axisymmetric with the window. Thus

$$I(r, z) \approx I(r) = I_p \exp(-r^2/2\sigma^2) , \quad (2)$$

where I_p is the peak power density of the incoming laser beam and σ is the beam radius, that is, at a radial distance of 2σ from beam center, the power density reduces to $e^{-2}I_p$. By dividing σ by the window radius a , the normalized beam radius σ_e is obtained. Then, Eq. (2) becomes in normalized coordinates:

$$I(\rho) = I_p \exp(-\rho^2/2\sigma_e^2) . \quad (3)$$

The relationship between σ_e , as defined here, and the beam-size parameter α^2 , introduced by Bendow and Gianino,³ is given by:

$$\alpha^2 = 1/4 \sigma_e^2 . \quad (4)$$

The total power contained within the incoming laser beam (P_l) is related to $I(r)$ in the following way:

$$P_l = \iint I(r) dA = \int_0^\infty I_p \exp(-r^2/2\sigma^2) 2\pi r dr = 2\pi\sigma^2 I_p , \quad (5)$$

with dA being the elemental surface area. Note that the integrals over the surface area cover all space. Solving for I_p gives:

$$I_p = P_l / 2\pi\sigma^2 \text{ or } P_l / 2\pi a^2 \sigma_e^2 . \quad (6)$$

Utilizing Eq. (6) in Eqs. (2) or (3) and multiplying by β , we get the steady-state volume heating source term as:

$$Q(r) = [\beta P_l / 2\pi\sigma^2] \exp(-r^2/2\sigma^2) , \quad (7)$$

or,

$$Q(\rho) = [\beta P_l / 2\pi a^2 \sigma_e^2] \exp(-\rho^2/2\sigma_e^2) . \quad (8)$$

However, in most experimental situations it is more convenient to measure transmitted power (P_t) rather than the incident laser power (P_l). Under the assumption that $\beta L \ll 1$, then these two quantities are related by:⁸

$$P_t/P_l = 2n/(n^2 + 1) \quad , \quad (9)$$

n being the refractive index of the medium. Solving for P_l :

$$P_l = P_t(n^2 + 1)/2n \quad . \quad (10)$$

In this work we have assumed that it will always be the quantity P_t that is known initially and the P_l will have to be computed via Eq. (10). Therefore, the computer program has been written to accept P_t as input and to transform to P_l according to the above formula.

The program is also capable of handling a z -dependence of the source term Q . This capability is discussed more fully in Section 11. Under this circumstance, the assumption of $\beta L \ll 1$ may not be valid, necessitating a more accurate formula for transmitted power P_t than that stated in Eq. (9).

3.3 The Boundary Condition Equation

As mentioned in Section 3.1, the window temperature distribution is also governed by the boundary conditions (BC) on its four surfaces. The BC Equation for the i th surface is of the form:⁹

$$K(\partial T_{s_i}/\partial p_i) = g_i - h_i T_{s_i} \quad , \quad (11)$$

where T_{s_i} is the temperature at the surface, h_i is the surface's heat transfer coefficient [$W/cm^2 - ^\circ C$], g_i is the total heat flux into the surface [W/cm^2] and $\partial/\partial p_i$ is the directional derivative along the normal pointing outward from the i th surface. The index i runs from 1 to 4. The inner and outer cylindrical surfaces located at r_1 and " a " are designated by the indices 1 and 2, respectively; whereas, the plane window faces located at $z = -L/2$ and $L/2$ are designated by the indices 3 and 4, respectively. There will be an equation of type (11) for each surface of the window, thereby allowing independent treatment of each boundary.

8. Weil, R. (1970) J. Appl. Phys. 41:3012; and Bendow, B., Hordvik, A., Lipson, H., and Skolnik, L. (1972) AFCRL-72-0404, unpublished, p. 12.

9. Carslaw, H. S., and Jaeger, J. C. (1959) Conduction of Heat in Solids, 2nd edition, Oxford Press, London, p. 19.

The terms on the right-hand side of Eq. (11) refer to the total flux of energy absorbed by the surface (g_i) and the total flux emitted ($h_i T$). Their difference is equal to the net flux absorbed by the surface, given by $K(\partial T_{S_i}/\partial p_i)$. The term g_i , in turn, has two contributors: the heat influx from the surrounding environment whose ambient temperature is T_a and that from additional external heat sources (F_i). That is,

$$g_i = h_i T_a + F_i \quad (12)$$

There are 4 common BC which typically characterize practically all of the surfaces of interest. They are:

(BC1) Insulated Surface: Since no radiation can enter or leave the surface, both g_i and h_i are set equal to zero.

(BC2) Given Heat Input: h_i is set equal to zero so that there will be no heat flow out of the surface. All of the heat influx from the external source originates from F_i , so that $K(\partial T_{S_i}/\partial p_i) = g_i = F_i$.

(BC3) No Thermal Constraints: Here, the surface is experiencing both an influx and efflux of heat radiation. In general, all of the terms in Eqs. (11) and (12) are present and are finite, although in the typical case F_i will usually be zero. The heat outflow is represented by $h_i T_{S_i}$, in which T_{S_i} is varying. Thus, the net flux absorbed is given typically by $h_i(T_a - T_{S_i})$. The condition usually known as Newton's Law⁹ occurs when $T_{S_i} > T_a$ and $F_i = 0$.

(BC4) Fixed Surface Temperature: To hold the surface temperature T_{S_i} fixed, h_i must be set equal to a large value in order that the surface may be an efficient dissipator of any additional heat reaching it. Furthermore, the temperature of the ambient environment in the immediate vicinity of the surface must be the same as that of the surface (that is, $T_a = T_{S_i}$) so that there will be no net exchange of energy between the two regions. Therefore, if we set $F_i = 0$, then $g_i = h_i T_a = h_i T_{S_i}$ and there is no net absorbed flux.

The information on all of the parameters pertaining to these four BC is tabulated in Table 1. Note that all of the BC of practical interest can be represented by an appropriate choice of g_i and h_i . This will allow the resulting computer program to be very flexible.

For the case in which the window is a full disc, then g_i and h_i (which pertain to the nonexistent inner cylindrical surface) are set equal to zero.

Table 1. Information on All the Parameters (g_i , h_i , F_i , T_a , T_{si}) for the Boundary Condition (BC) Equation

| BC | g_i | h_i | F_i | T_a | T_{si} | Net Flux Absorbed |
|----|-----------------|--------|--------|----------------|----------|----------------------|
| 1 | 0 | 0 | 0 | — | varies | 0 |
| 2 | F_i | 0 | finite | — | varies | F_i |
| 3 | $h_i T_a + F_i$ | finite | finite | fixed | varies | $h_i (T_a - T_{si})$ |
| 4 | $h_i T_{si}$ | large | 0 | $T_a = T_{si}$ | fixed | 0 |

4. THE FAR-FIELD INTENSITY PATTERN

Originally, the TEMP5 (heat) program was written to solve the heat and BC equations when they were in a nondimensional form. Consequently, its results (temperatures throughout the window) would be expressed in nondimensional form. On the other hand, the TIKIRK (optical) program was designed to work with actual (that is, dimensioned) quantities. To rectify this discrepancy, the TIKIRK program has been written to accept all of the normalized output from TEMP5 and to dimensionalize it accordingly before using it. Thus, whenever these two programs are to be used together, only the normalized data from the TEMP5 program can be utilized. We have already indicated the transformations between the spatial coordinates r, z and ρ, ξ . The real time t and real temperature T are related to their nondimensional counterparts τ and w , respectively, via:

$$\tau = \kappa t / a^2 \quad (13)$$

$$w = T / \Delta T_c \quad (14)$$

where

$$\Delta T_c = \beta P_f / K\pi \quad (15)$$

Before the temperature output of TEMP5 — in the form of $w(\rho, \xi, \tau)$ — is fed into TIKIRK, it is integrated over the thickness of the window to obtain:

$$F1(\rho, \tau) = \int_{\xi_1}^{\xi_2} w(\rho, \xi, \tau) d\xi \quad (16)$$

Another function, F2, is obtained from F1 via:

$$F2(\rho, \tau) = \rho^{-2} \int_0^{\rho} F1(\rho, \tau) \rho \, d\rho \quad (17)$$

The dimensionless functions F1 and F2 can be converted to real time t by means of Eq. (13). Knowing these two F-functions, one can determine the time-dependent aberration functions $\Phi^{\rho, \theta}$ associated with the ρ - and θ - polarized waves.⁴ These Φ -functions contain all of the material properties of the window and characterize its thermal stresses as functions of time. They are of the form:

$$\Phi^{\gamma}(\rho, t) = a \Delta T_c \left[S_1^{\gamma} F1(\rho, t) + 4 S_2^{\gamma} F2(\rho, t) \right] \quad , \quad (\gamma = \rho, \theta) \quad (18)$$

The S_j^{γ} are the thermal lensing parameters, defined as:⁴

$$S_1^{\rho} = dn/dT + \bar{\alpha} n^3 [(1 - \nu) p_{12} - \nu p_{11}] / 2 + \bar{\alpha} (1 + \nu)(n - 1) \quad (19)$$

$$S_2^{\rho} = -S_2^{\theta} = \bar{\alpha} n^3 (1 + \nu)(p_{11} - p_{12}) / 8 \quad (20)$$

$$S_1^{\theta} = dn/dT + \bar{\alpha} n^3 [p_{11} - 2\nu p_{12}] / 2 + \bar{\alpha} (1 + \nu)(n - 1) \quad , \quad (21)$$

where dn/dT is the temperature derivative of refractive index, $\bar{\alpha}$ is the thermal expansion coefficient, ν is Poisson's ratio and the p_{ij} are the Pockels elastooptic coefficients.* These S_j^{γ} must be calculated in advance and read in as input since the program does not compute them.

*The terms containing the elastooptic coefficients in Eqs. (19) through (21) represent the "isotropic approximation" commonly utilized in the literature for crystalline windows, but which is, strictly speaking, valid only for amorphous solids. When the effects of crystallinity are taken into account, the forms of the above elastooptic terms can change significantly. For example, F. Horrigan of Raytheon Corp. and, later, J. Marburger and M. Flannery of the University of Southern California, have considered the case of a single crystal window whose face is a {111} plane and communicated their somewhat different results to us. The elastooptic terms based on Horrigan's work have been reported in B. Bendow, P. Gianino, Y. Tsay and S. Mitra, Appl. Opt. 13, 2382 (1974), [Eq. (33)]. The corresponding terms based on the Marburger-Flannery analysis have been reported in B. Bendow and P. Gianino, Appl. Opt. 14, 277 (1975), [Eq. (3)]. The results for the effective p_{ij} 's to be utilized for polycrystalline media are given by M. Flannery and J. Marburger, Proc. of Fifth Conf. on IR Laser Window Materials, C.R. Andrews and C.L. Strecker, Editors, ARPA, Arlington, Virginia (1976), p. 781.

Since the S_j^γ have dimensions of $(^\circ\text{C})^{-1}$, then the Φ^γ will be expressed in cm.

Previously,^{2, 4, 5} we determined the transmitted intensity at a field point in space for an unpolarized beam with an axisymmetric Gaussian distribution incident on the window. The field point in space is specified by the cylindrical coordinates X, ρ' , in which X is the distance from the window's center measured along an axis orthogonal to the plane of the window and through its center, while ρ' is the perpendicular radial distance from this line to the field point. The Gaussian focal distance, that is, the axial distance from the window's center to the Gaussian focal point, is given by X_0 . These coordinates are shown in Figure 2. Since the spatial intensity pattern is circularly symmetrical about this axial line, there is no dependence on the cylindrical angular coordinate.

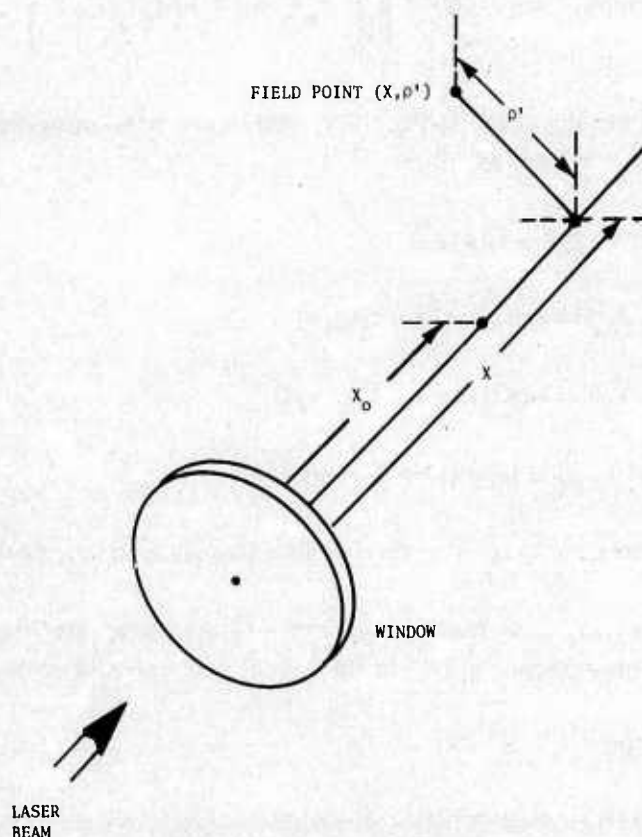


Figure 2. Cylindrical Coordinates for the Field Point in Space. The origin is at the center of the window. X_0 is the Gaussian focal distance

Sometimes, rather than using the dimensioned coordinates X and ρ' , it is advantageous to employ the nondimensional generalized coordinates u and v in the calculation of the intensity. These coordinates are measured from the Gaussian focal point and are closely related to the "optical coordinates" of Born and Wolf.¹⁰ Specifically,

$$u = ka^2(X_0^{-1} - X^{-1}) \quad , \quad v = ka\rho'/X \quad , \quad (22)$$

where k is the wave number $2\pi/\lambda$, and, λ is the wavelength. (At the Gaussian focus both u and v vanish, by definition, so $X = X_0$, $\rho' = 0$). Specifically, the intensity at a given point u, v in the far field at any time t relative to the intensity at the Gaussian focus at zero time is given by:²⁻⁶

$$I'(u, v, t) = 2\alpha^4(1 - \exp(-\alpha^2))^{-2} \left\{ \left| \int_0^1 f_w f_x d\rho \right|^2 + \left| \int_0^1 f_w f_y d\rho \right|^2 \right\} . \quad (23)$$

The functions within the brace in Eq. (23), which are to be integrated over the window's face, are defined as follows:

$$f_w(\rho, u) = \exp(-\alpha^2 \rho^2 - iu\rho^2/2) \quad , \quad (24)$$

$$f_x(\rho, v, t) = \rho J_0(\rho v) \exp(ik\Phi^0) - f_z(\rho, v, t) \quad , \quad (25)$$

$$f_y(\rho, v, t) = \rho J_0(\rho v) \exp(ik\Phi^0) + f_z(\rho, v, t) \quad , \quad (26)$$

$$f_z(\rho, v, t) = v^{-1} J_1(\rho v) [\exp(ik\Phi^0) - \exp(ik\Phi^0)] \quad , \quad (27)$$

where J_0 and J_1 are the zero- and first-order Bessel functions of the first kind, respectively.

Usually, however, it is desirable to express the above intensity in terms of the dimensioned coordinates X, ρ' . In that case, the intensity is determined by:

$$I(X, \rho', t) = I'(u, v, t) \cdot X_0^2/(X^2 + \rho'^2) \quad . \quad (28)$$

It will be the objective of the TIKIRK program to compute Eqs. (23) through (28).

10. Born, M., and Wolf, E. (1964) Principles of Optics, 2nd (revised) edition, Macmillan Co., New York, p. 437.

Before pursuing the solutions to the heat and diffraction problems, it would serve our convenience if we paused to classify the input parameters into categories which describe the window's geometry, its material composition, surface characteristics and the beam properties:

Geometrical Parameters: a, L, r_1

Material Parameters: $n, \beta, K, c_p, d, S_j^*$

Surface Parameters: g_i, h_i

Beam Parameters: σ, P_t, λ

5. THE PROGRAMMED FORMS OF THE HEAT AND BC EQUATIONS

5.1 Nondimensional Form

The heat and BC equations can be cast into a nondimensional form by dividing Eq. (1) by $\kappa \Delta T_c / a^2$ and Eq. (11) by $K \Delta T_c / a$, obtaining:

$$\partial w / \partial t = \nabla_{\rho, \xi}^2 w + (2\sigma_e^2)^{-1} \exp(-\rho^2 / 2\sigma_e^2) \quad (29)$$

and

$$\partial w_{s_i} / \partial (p_i / a) = a g_i / K \Delta T_c - (a h_i / K) w_{s_i} \quad (30)$$

in which use has been made of the normalized distances, plus Eqs. (13), (14), (15), and (10). Rewriting these equations in terms of the notation used in the computer program (that is, the quantities printed out), there results:

$$\partial U / \partial (TAU) = \nabla_{(RHO), (ZED)}^2 U + A \exp \{ - (RHO)^2 / 2(SIG)^2 \} \quad (31)$$

$$\partial U_{Si} / \partial \eta_i = G1(i) - H1(i) \cdot U_{Si} \quad (32)$$

where

$$\nabla_{(RHO), (ZED)}^2 \equiv (RHO)^{-1} \partial / \partial (RHO) \{ (RHO) \partial / \partial (RHO) \} + \partial^2 / \partial (ZED)^2$$

The integration on RHO proceeds from RHO1 to RHO12, while that on ZED goes from $-|ZED1|$ to $|ZED1|$.

Upon comparing Eqs. (31) and (32) with (29) and (30), respectively, one can make the following associations:

$$\begin{aligned}
 U &\equiv w \\
 \text{TAU} &\equiv \tau \\
 \text{RHO} &\equiv \rho \\
 \text{ZED} &\equiv \xi \\
 \text{RHO1} &\equiv \rho_1 \\
 \text{RHO12} &\equiv \rho_{12} \\
 \text{ZED1} &\equiv \xi_1 \\
 A &\equiv 1/2 \sigma_e^2 \\
 \text{SIG} &\equiv \sigma_e \\
 G1(i) &\equiv a g_i / K \Delta T_c \\
 H1(i) &\equiv a h_i / K
 \end{aligned} \tag{33}$$

$\eta_i \equiv p_i/a$ and refers to the normalized coordinates ρ or ξ , depending upon the surface being considered. We emphasize, once again, that the computer variable quantities on the left of Eqs. (33) are those printed out by the program, while those quantities on the right represent the interpretations that are to be given to the computer variables. Note that all of these quantities are normalized so as to be dimensionless. The interpretation delineated in Eq. (33) is mandatory when the TEMP5 program is to be used as a predecessor to the TIKIRK program or when temperature plots are to be made.

A perusal of the right hand sides of Eqs. (33) shows that one must know all of the geometrical, material, surface and beam parameters listed in the previous section (except S_j^γ and λ) in order to specify completely the computer variables on the left sides of Eqs. (33). For the case of no volume source, the last term in the heat equation vanishes, obviating the need for SIG and A. (A control to bypass this term is available in the program.)

5.2 A Dimensioned Form

For those situations in which one wants only the numerical results of the real temperature distribution throughout the window as a function of real space and time, but not the diffracted laser beam intensity, a different arrangement of the heat and BC equations can be formulated, resulting in a more convenient (dimensioned) interpretation of the computer variables. Here, Eq. (1) is divided by κ and Eq. (11) by K , obtaining:

$$\partial T / \partial \tau' = \nabla_{r,z}^2 T + (\Delta T_c / 2\sigma^2) \exp(-r^2 / 2\sigma^2) \quad (34)$$

and

$$\partial T_{s_i} / \partial p_i = g_i / K - (h_i / K) T_{s_i} \quad (35)$$

in which Eqs. (15) and (9) have been used, and,

$$\tau' \equiv \kappa t \text{ [cm}^2\text{]} \quad (36)$$

Again, Eqs. (34) and (35) must be compared to the computerized forms, Eqs. (31) and (32), respectively, resulting in the following new associations for the printed output:

$$\begin{array}{lll} U & \equiv T & [^{\circ}\text{C}] \\ \text{TAU} & \equiv \tau' & [\text{cm}^2] \\ \text{RHO} & \equiv r & [\text{cm}] \\ \text{ZED} & \equiv z & [\text{cm}] \\ \text{RHO1} & \equiv r_1 & [\text{cm}] \\ \text{RHO12} & \equiv a - r_1 & [\text{cm}] \\ \text{ZED1} & \equiv -L/2 & [\text{cm}] \\ A & \equiv \Delta T_c / 2\sigma^2 & [^{\circ}\text{C}/\text{cm}^2] \\ \text{SIG} & \equiv \sigma & [\text{cm}] \\ G1(i) & \equiv g_i / K & [^{\circ}\text{C}/\text{cm}] \\ H1(i) & \equiv h_i / K & [\text{cm}^{-1}] \end{array} \quad (37)$$

$\eta_i \equiv p_i$ and refers to either r or z , depending upon the surface being considered. Again, the terms on the left of Eqs. (37) are the computer variables, while those on the right are their physical interpretations. From an inspection of Eqs. (37), it is obvious that the temperature as well as all distances and lengths are given in their accustomed units; whereas the time (TAU), volume heating source (A) and the surface parameters (G1(i) and H1(i)) are not.

Once again, a perusal of the right hand sides of Eqs. (37) points out that one must know all of the required parameters, except S_j^y and λ , in order to specify completely the computer variables on the left sides of Eqs. (37). As before, if there is no volume source, SIG and A also become unnecessary.

6. GRAPHS FOR TWO MODEL PROBLEMS

6.1 Description of the Models

The DISPLAY program has the capability of exhibiting the distributions of the temperature (T) and the intensity (I) in a variety of ways. For both T and I the program can provide three different types of displays, viz, plots of contour maps, perspective views which give a three-dimensional effect, and multiple cross-sections through these perspective views which are parallel to the coordinate axes. In this section, we present various examples of each kind of plot for two model problems. These plots were produced on the AFGL Calcomp plotter associated with the CDC6600 computer.

The first model chosen (Model No. 1) consisted of a disc-shaped cylindrical window of ZnSe. It was 1.3 cm thick and had a radius of 30 cm. The entrance face (at $z = -0.65$ cm) and the outer rim were maintained at a fixed temperature of 0°C , while the exit face (at $z = +0.65$ cm) was held at -100°C . Thus, the three surfaces satisfied BC No. 4 (see Table 1). The remainder of the window was initially at 0°C in an ambient atmosphere also at 0°C . In order to insure adequate removal of heat at the three surfaces so that these temperatures could be maintained, the surfaces' heat transfer coefficients ($h_i, i=2, 3, 4$) were set equal to the arbitrarily large value of $6 \times 10^{12} \text{ W/cm}^2 - ^\circ\text{C}$. From Table 1, the total surface flux is $g_i = h_i T_{s_i}$. Therefore, $g_2 = g_3 = 0$, while $g_4 = h_4 T_{s_4} = -6 \times 10^{14} \text{ W/cm}^2$. The normalized radius of the laser beam irradiating the window was given by $\sigma_e = 0.289$ (corresponding to $\alpha^2 = 3$).

The second model (Model No. 2) consisted of an annular-shaped cylindrical window of ZnSe, having the same thickness and outer radius as that in Model No. 1, but with an inner radius of 7.5 cm. The same laser beam was assumed here also. The inner edge of this annulus was fixed at -100°C . Its surface heat transfer coefficient was set at $10^4 \text{ W/cm}^2 - ^\circ\text{C}$, with $g_1 = -10^6 \text{ W/cm}^2$ (BC No. 4). The other three surfaces were left free to radiate in accordance with Newton's law, each having transfer coefficients of $10^{-2} \text{ W/cm}^2 - ^\circ\text{C}$ (BC No. 3). The remainder of the window was initially at 0°C . The ambient atmospheric temperature about the latter three surfaces was 0°C , resulting in $g_2 = g_3 = g_4 = 0$; while that in the vicinity of the inner surface was -100°C .

6.2 Multiple X-Y Plots

6.2.1 X-Y TEMPERATURE PLOTS

For multiple plots involving the temperature, one may graph temperature either as a function of (dimensioned) axial distance (z) through the window at a constant (dimensioned) radial position (r), or, as a function of radial distance at

a constant axial position. We arbitrarily classify the first type as a "Y-plot," the second as an "X-plot."

Examples of both kinds of these plots are shown in Figures 3 to 11. Figures 3 to 6 are of the Y-type for the case of Model No. 1; Figures 7 to 11 are of the X-type, of which Figures 7 to 9 pertain to Model No. 1, while Figures 10 and 11 pertain to Model No. 2. On all of these X-type plots, the (dimensioned) radial distance is labelled "RHO." Also included in the caption of each figure is the appropriate plot command required to construct the graph. This plot command will be explained fully in Volume II, Section 10. Figure 3 is an example of T versus z through the center line of the window, that is, $r = 0$, for the 9 times listed on the right hand side of the graph. To the left of the graph are listed many of the TEMP5 parameters of interest (see Table 2, Volume II). All of these parameters involving RHO's, ZED's, TAU's, G1's and H1's are the normalized terms enumerated on the left hand sides of Eqs. (33); whereas, the quantities from BETA and below are listed with their actual dimensioned values.

In Figures 4 and 5, T versus z is plotted at constant radial distances of 15 and 30 cm, respectively, for the same 9 times as in Figure 3.

Figures 3, 4, and 5 are examples of cases in which r was held fixed for each given plot. Figure 6 is an example of how the parametric values of r can be varied within one given plot. Here, T is plotted against z for the 3 different radial positions of 0, 15 and 30 cm at the fixed time of 5 sec.

In Figures 7A and B the temperature is plotted against r in 21 different axial positions (or planes) for time values of 1 and 5 sec, respectively. Two of these planes are singled out in Figures 8 and 9, viz, the one which is 0.338 cm to the left of the window's center and the one 0.307 cm to the right, respectively. These planes occur approximately 1/4 and 3/4 of the way through the window, respectively. In both graphs, T is plotted against r for the 9 times shown.

Figures 10 and 11 are quite similar to Figures 8 and 9, except that Model No. 2 (that is, the annular window) was used and that the two planes selected occurred approximately at the window's center and at the exit face, respectively. Many of the TEMP5 parameters of interest are enumerated on the left side of Figure 10.

6.2.2 X-Y INTENSITY PLOTS

For multiple plots involving the intensity, one may plot intensity either as a function of axial distance in the far field at a constant radial position, or, as a function of radial distance at a constant axial position. (See Figure 2 for a clarification of axial and radial coordinates in the far field). A control exists in the program so that the axial and radial coordinates referred to here may be either the dimensioned quantities X and ρ' , or, the nondimensioned quantities u and v (see Section 4). As before, we classify the I-versus-X(or u) type of graph as a "Y-plot" and the

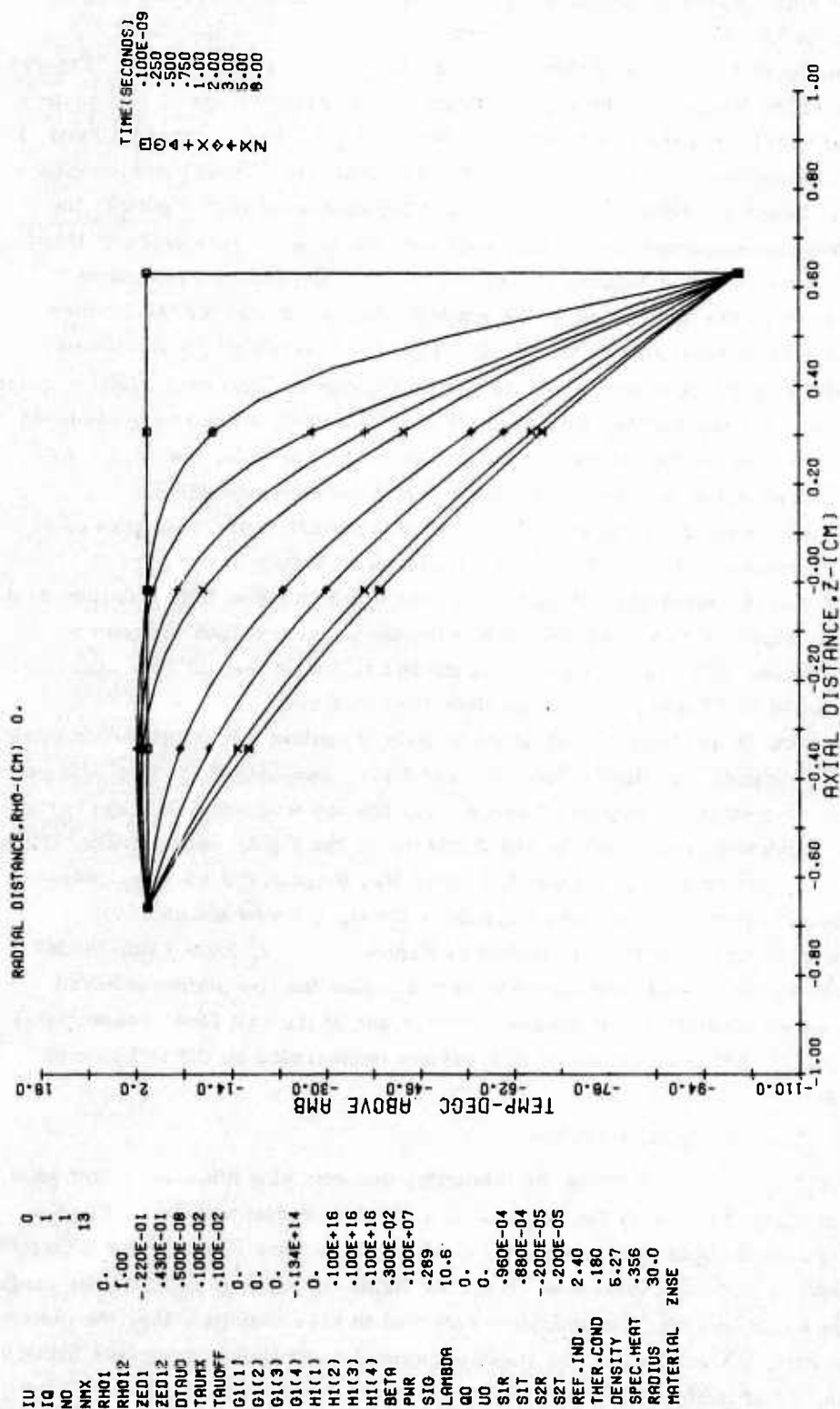


Figure 3. Temperature Versus Axial Distance in the Window at Zero Radial Position at the 9 Times Indicated, Using Model No. 1. Plot command is PLOT (1, 1, Y, 100, 1, NAS)

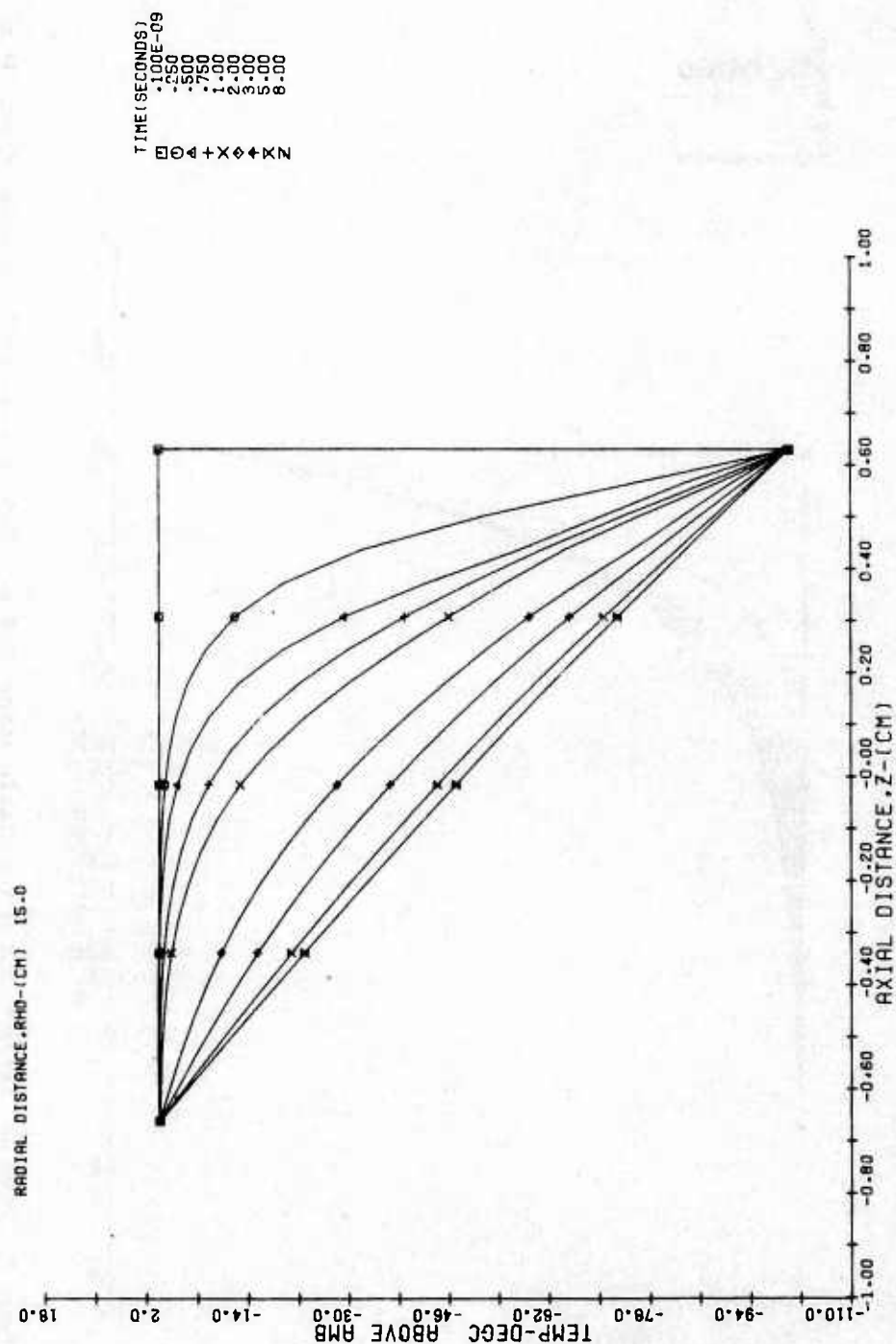


Figure 4. Same as Figure 3, but at a Radial Distance of 15 cm. Plot command is PLOT (1, 1, Y, 100, 41, NAS)

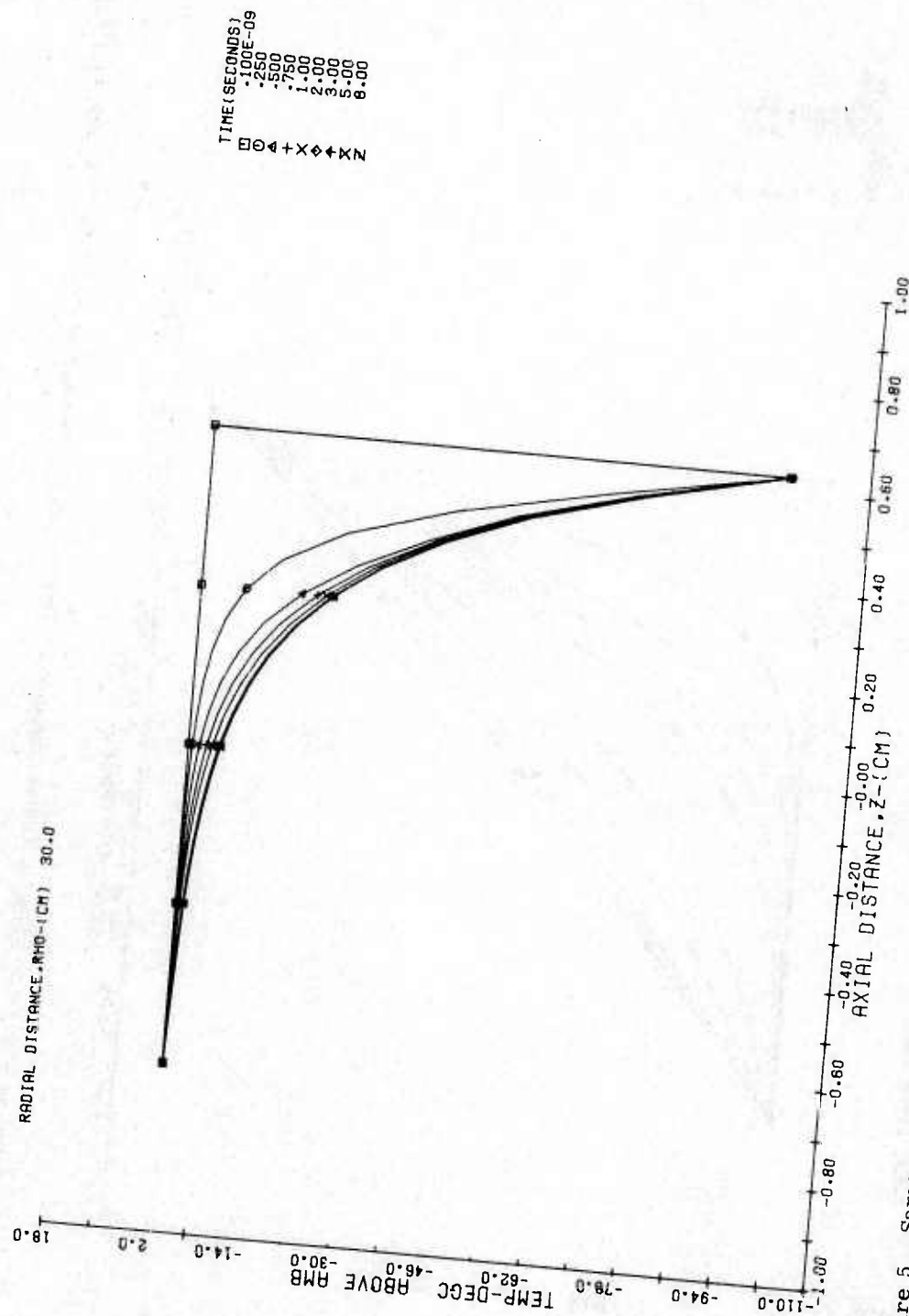


Figure 5. Same as Figure 3, but at a Radial Distance of 30 cm, that is, Just Inside the Outer Edge. Plot command is PLOT (1, 1, Y, 100, 81, NAS)

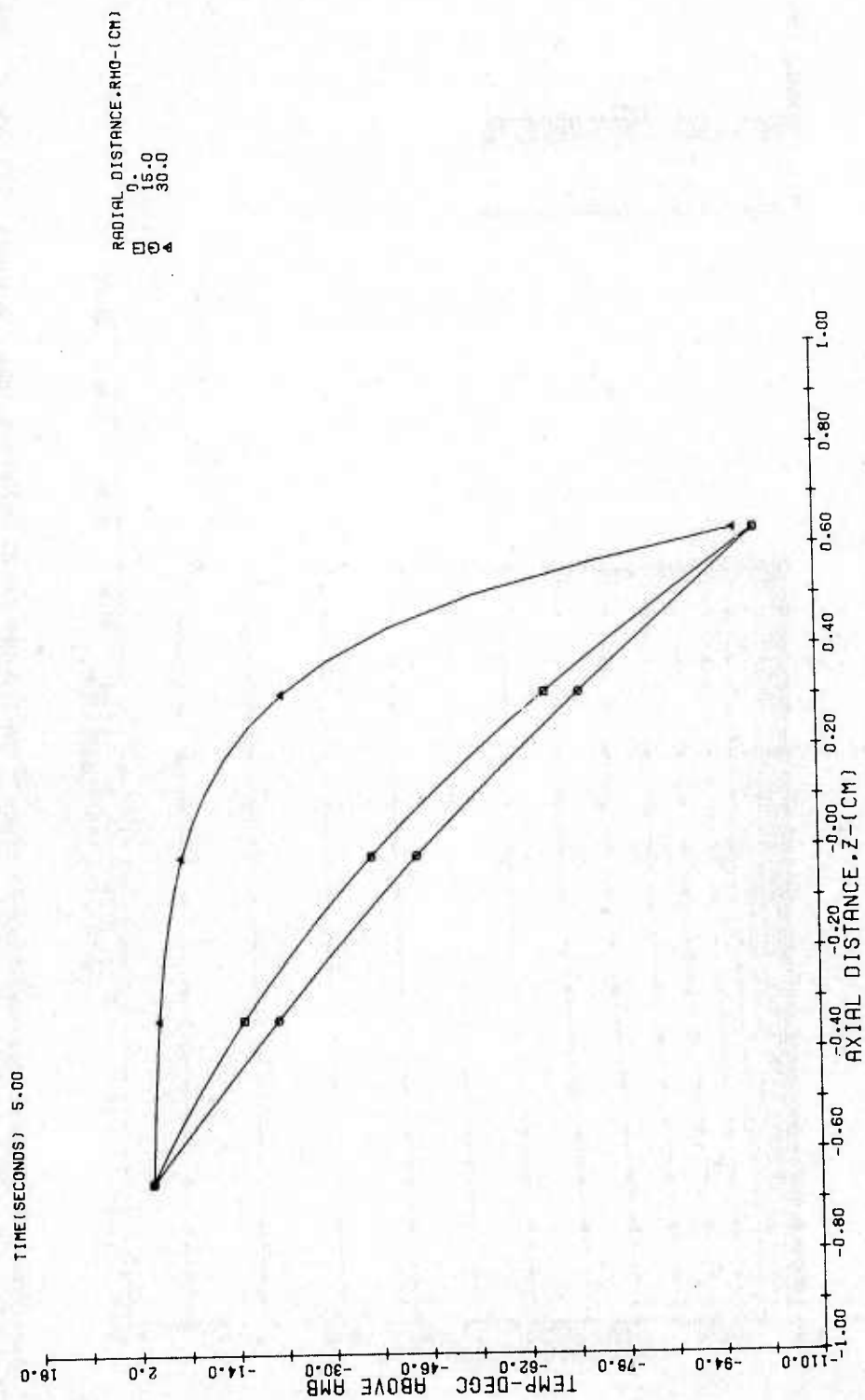


Figure 6. Temperature Versus Axial Distance in the Window for 3 Different Radial Positions at $t = 5$ sec, Using Model No. 1. Plot command is PLOT (4, 8, Y, 40, 1, NA)

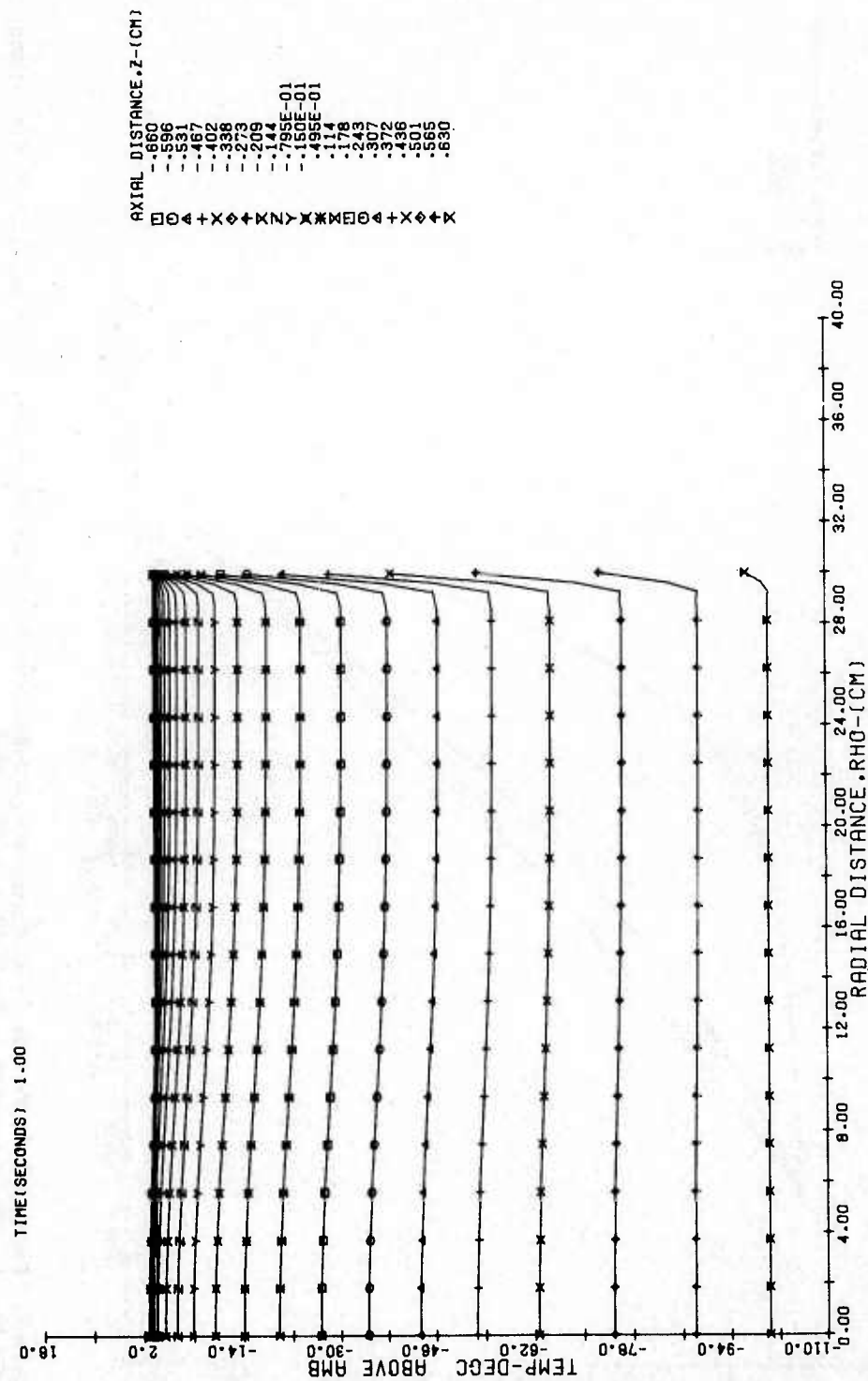


Figure 7A. Temperature Versus Radial Distance in the Window for 21 Different Axial Positions at Times of 1 Sec. Model No. 1 was Used. Plot Command is PLOT (3, 5, X, 1, 1, NA)

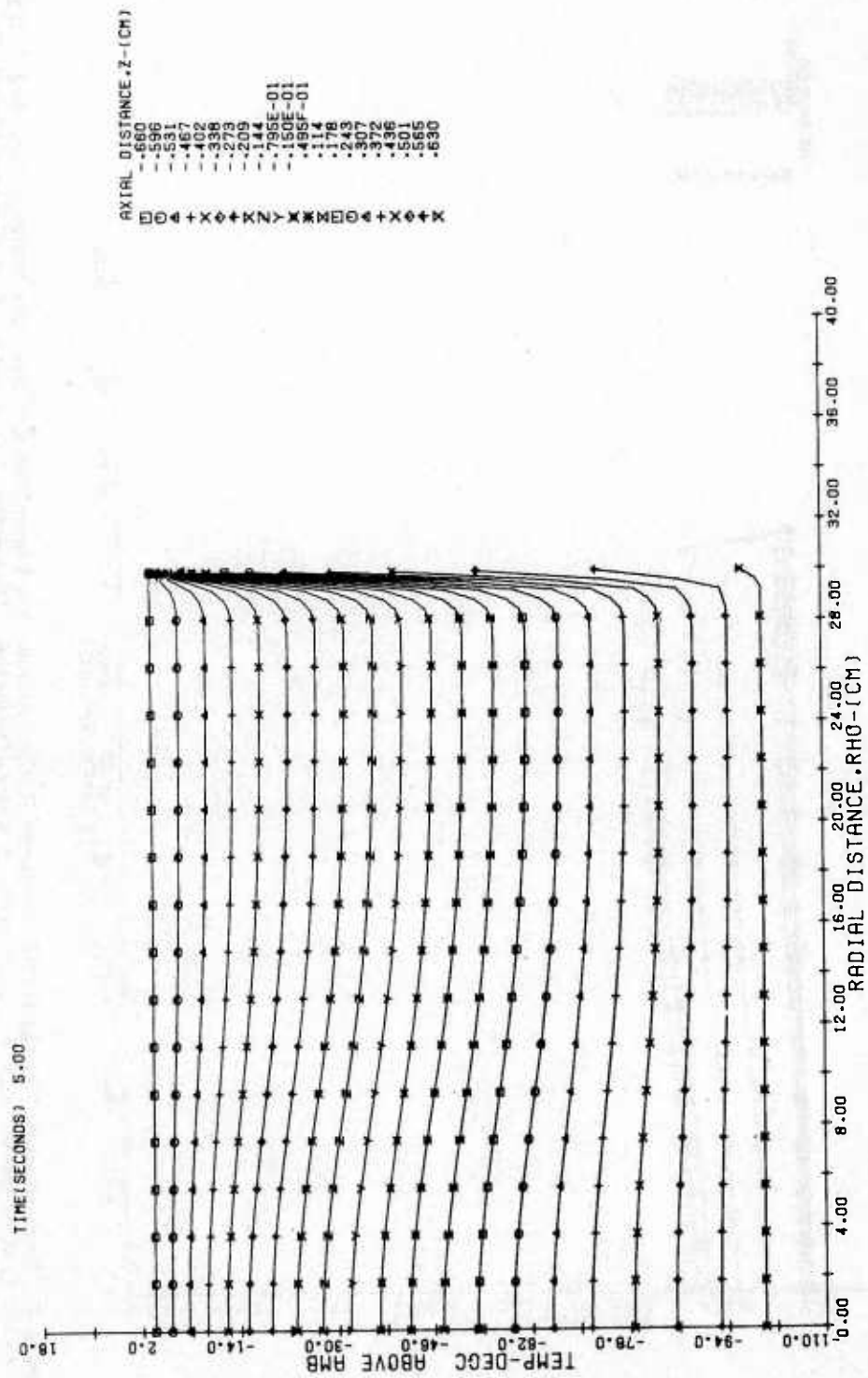


Figure 7B. Temperature Versus Radial Distance in the Window for 21 Different Axial Positions at Times of 5 Sec. Model No. 1 was Used. Plot Command is PLOT (3, 5, X, 1, 1, NA)

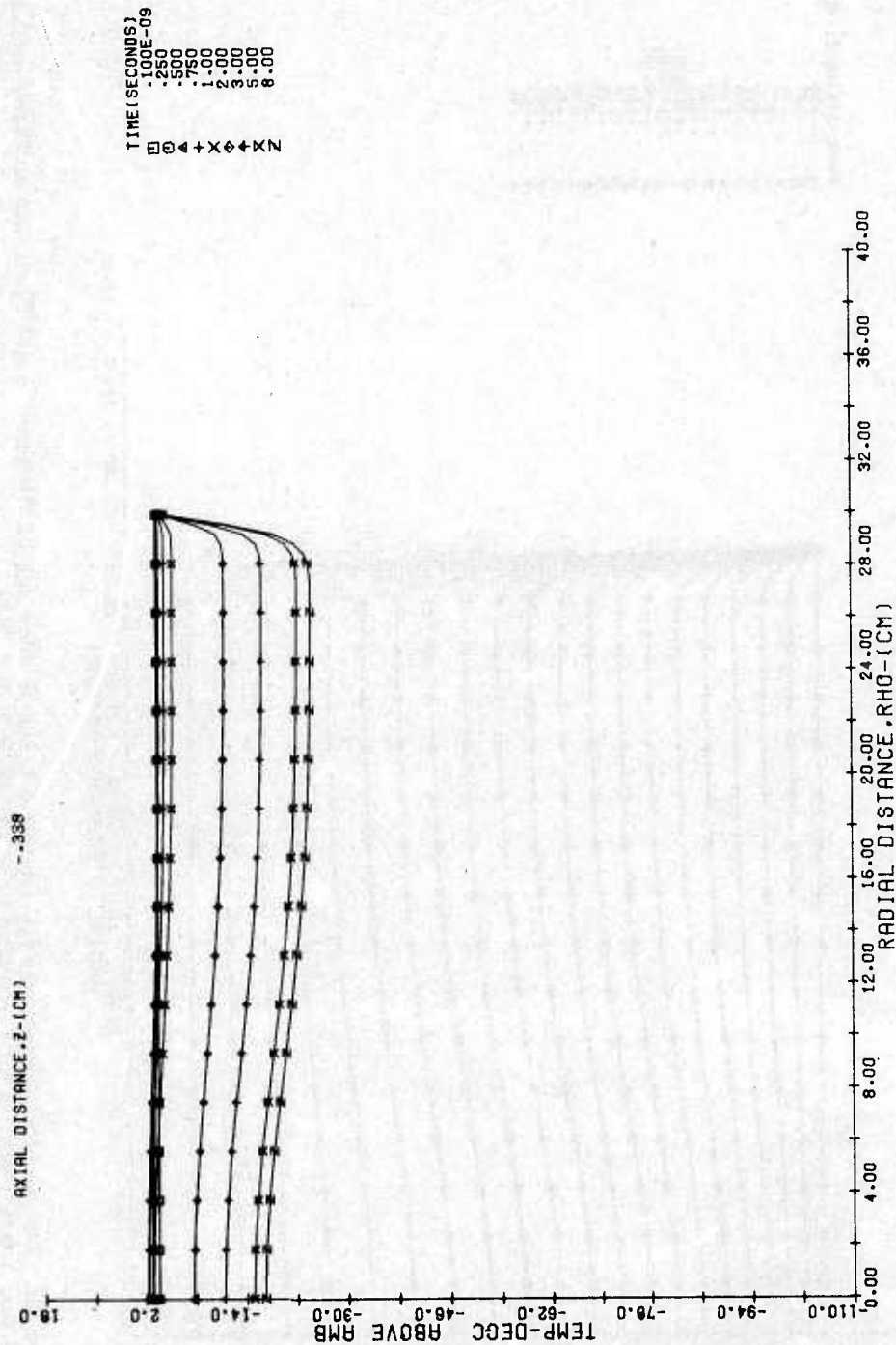


Figure 8. Temperature Versus Radial Distance in the Window in a Plane Through the Axis Which is Located 0.338 cm to the Left of the Window's Center at the 9 Times Indicated. Model No. 1 was used. Plot command is PLOT (1, 1, X, 100, 6, NAS)

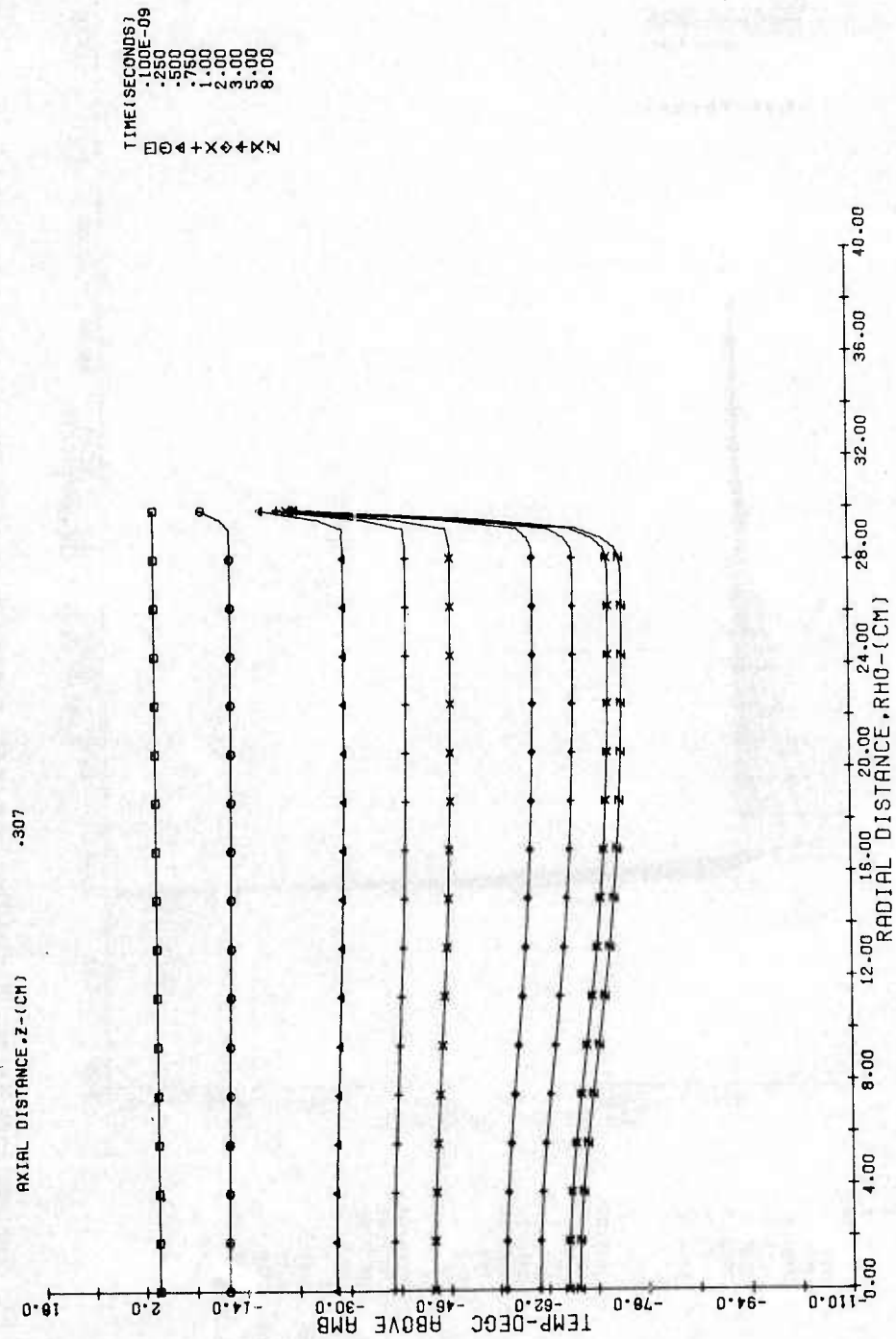


Figure 9. Same as Figure 8, Except That the Plane is Located 0.307 cm to the Right of the Window's Center. Plot command is PLOT (1, 1, X, 100, 16, NAS)

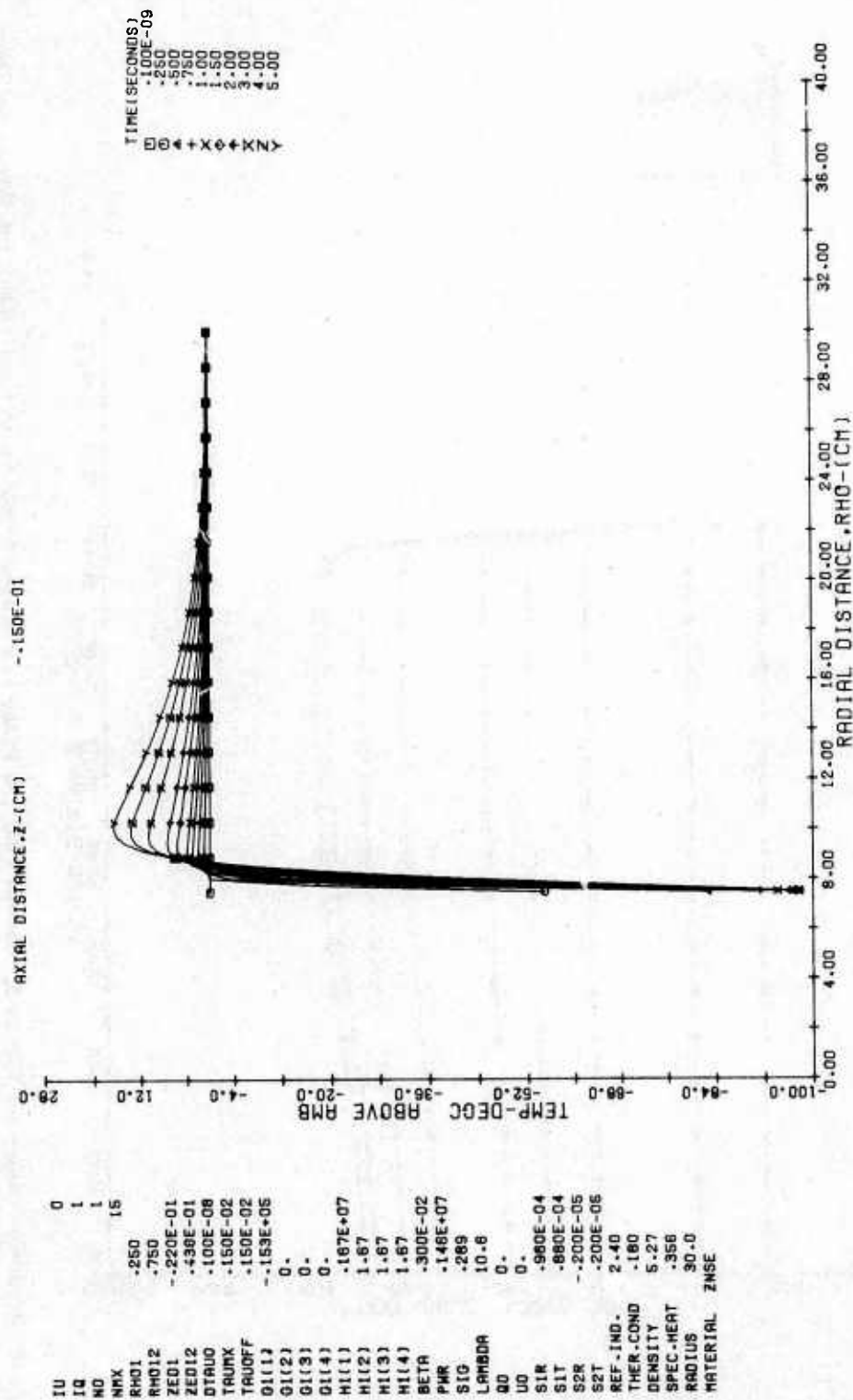


Figure 10. Temperature Versus Radial Distance in the Window in an Axial Plane Approximately Through the Window's Center at the 9 Times Indicated. Model No. 2 was used. Plot command is PLOT (1, 1, X, 100, 11, NAS)

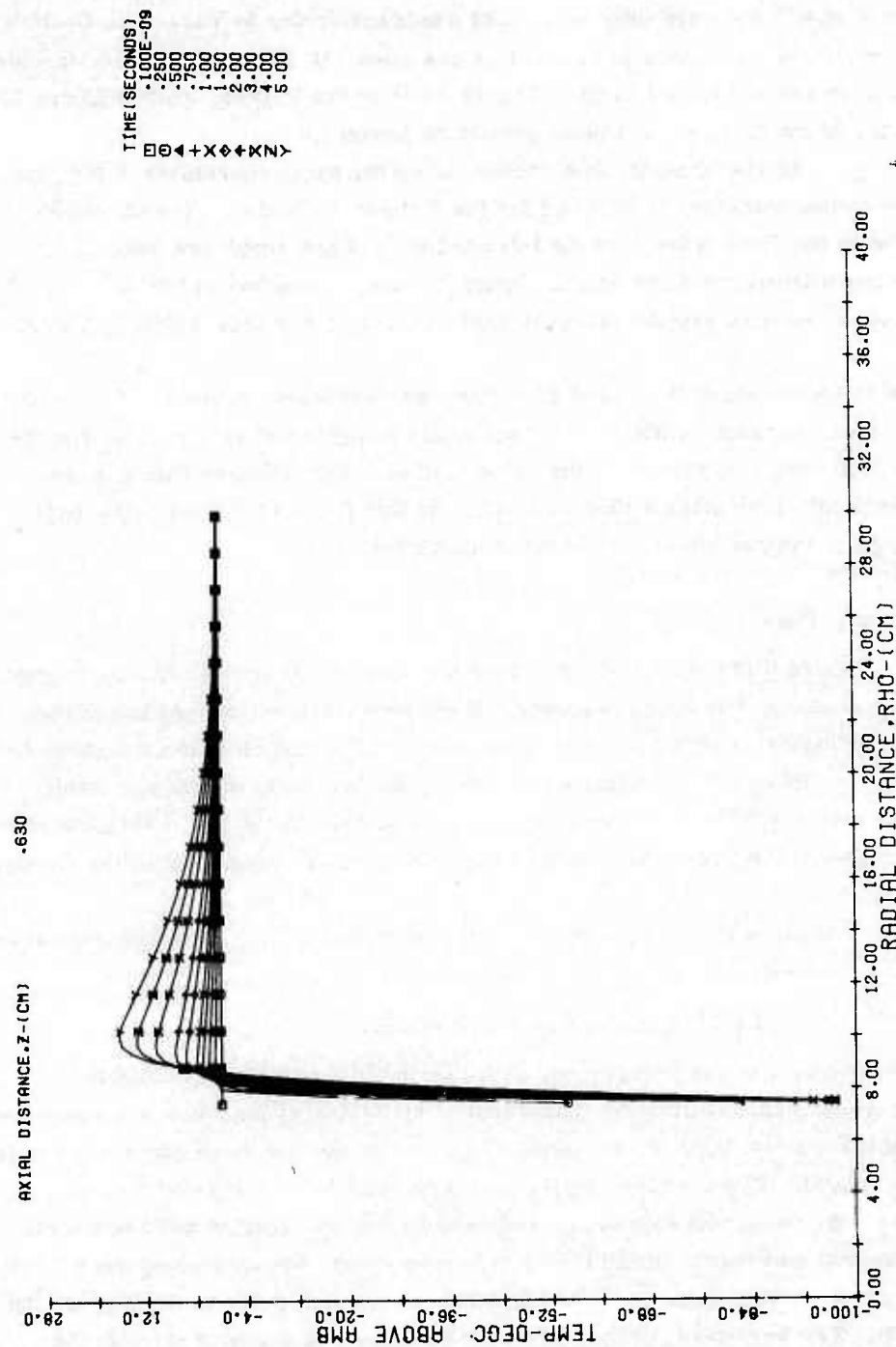


Figure 11. Same as Figure 10, Except That the Plane is Located Just Inside the Window's Exit Face. Plot command is PLOT (1, 1, X, 100, 21, NAS)

I-versus- ρ' (or v) as an "X-plot." However, this latter X is only a code symbol and should not be confused with the cylindrical coordinate X depicted in Figure 2. The code symbols X and Y are used only in the plot command (refer to Volume II, Section 10).

Examples of both kinds of these plots are shown in Figures 12 to 14, in which all distances are measured in cm. Figure 12 is of the Y-type, while Figures 13 and 14 are of the X-type. All plots pertain to Model No. 1.

In Figure 12 the intensity distribution along the axial coordinate itself (that is, zero radial distance) is depicted for the 9 times indicated. The quantities cataloged in the first column on the left hand side of the graph are the same TEMP5 parameters as displayed in Figure 3; those appearing in the upper portion of the second column are the relevant TIKIRK parameters (see Table 4, Volume II).

The intensity along the radial direction, perpendicular to the axial coordinate and at a fixed distance of 800 m along the axis, is exhibited in Figure 13 for the 9 times indicated. In Figure 14 the same kind of information is shown in the Gaussian focal plane after a time of 3 sec. At this particular time, this focal plane is occurring at a distance of 830 m along the axis.

6.3 Perspective Plots

Perspective plots are intended to give the viewer a three-dimensional aspect of the physical quantity being observed. Each perspective plot consists of two parts: a calibrated rectangular frame (to indicate the ranges of the distances being covered) with an arrow (to indicate the viewing angle), and, the 3D plot itself. The two "horizontal" coordinates of the 3D plot pertain to the two orthogonal distances involved; the "vertical" coordinate pertains to the magnitude of the physical quantity.

We now show perspective plots for both temperature in the window and intensity in the far field.

6.3.1 PERSPECTIVE TEMPERATURE PLOTS

The first part of the perspective temperature plot exhibits a calibrated rectangular frame representing the transverse rectangular cross-section through the center of the window (that is, the plane of the cross-section is perpendicular to the window's faces). The borders of the frame are parallel to the ρ and z axes. Because of the rotational symmetry, only one half of the section need be shown. The horizontal coordinate of the frame refers to radial distance along the window starting from its center (at the left end of the frame) and going to its edge (at the right end). The vertical coordinate represents the axial distance through the window, starting from the entrance face (bottom horizontal line) and going to the exit face (top horizontal line). The arrow above the frame shows the angle at

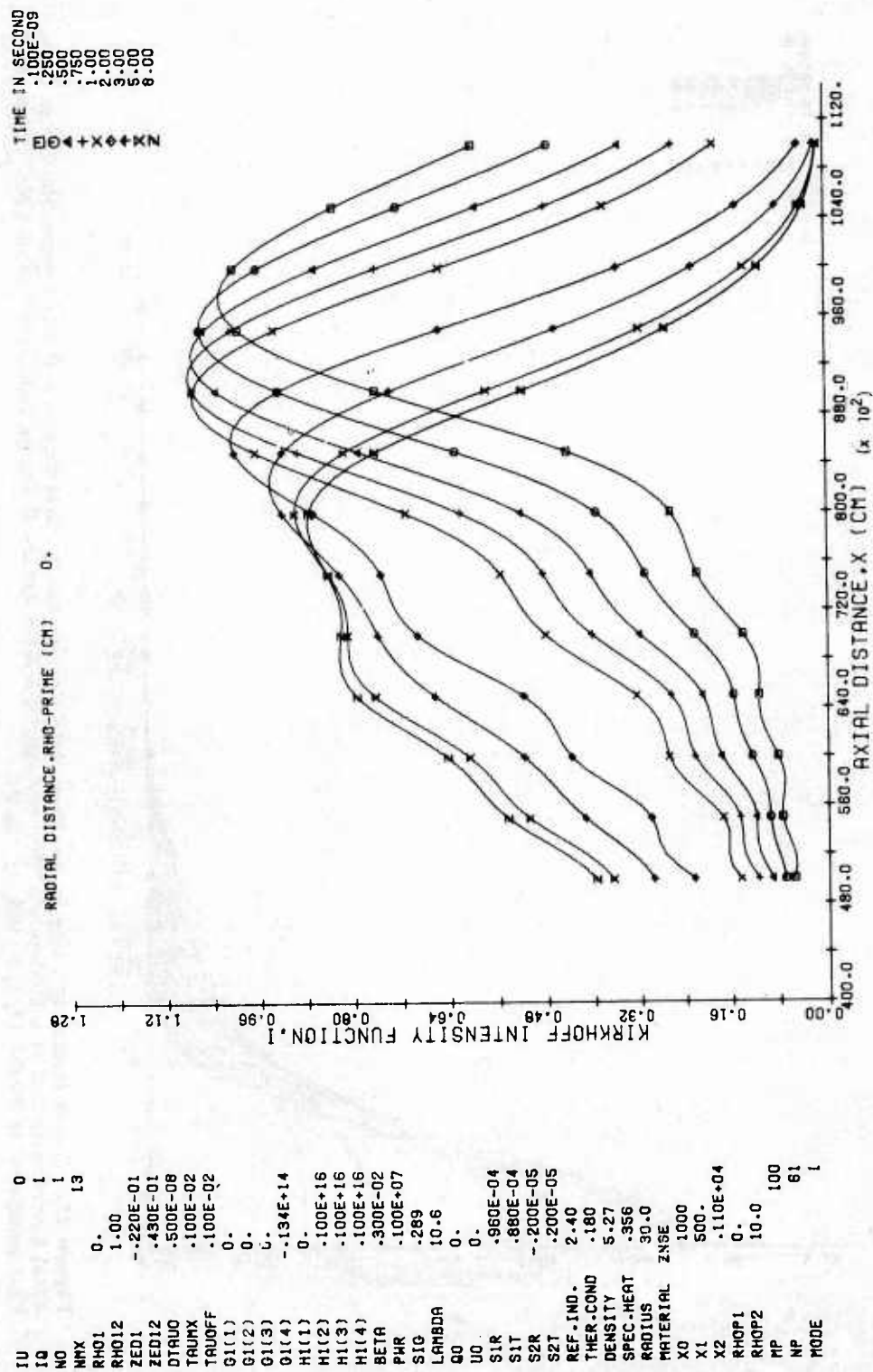


Figure 12. Laser Beam Intensity in the Far Field Versus Axial Distance Along the Axial Coordinate Itself (Zero Radial Distance) at the 9 Times Indicated, Using Model No. 1. Plot command is PLOT (1, 1, Y, 100, 1, NAS)

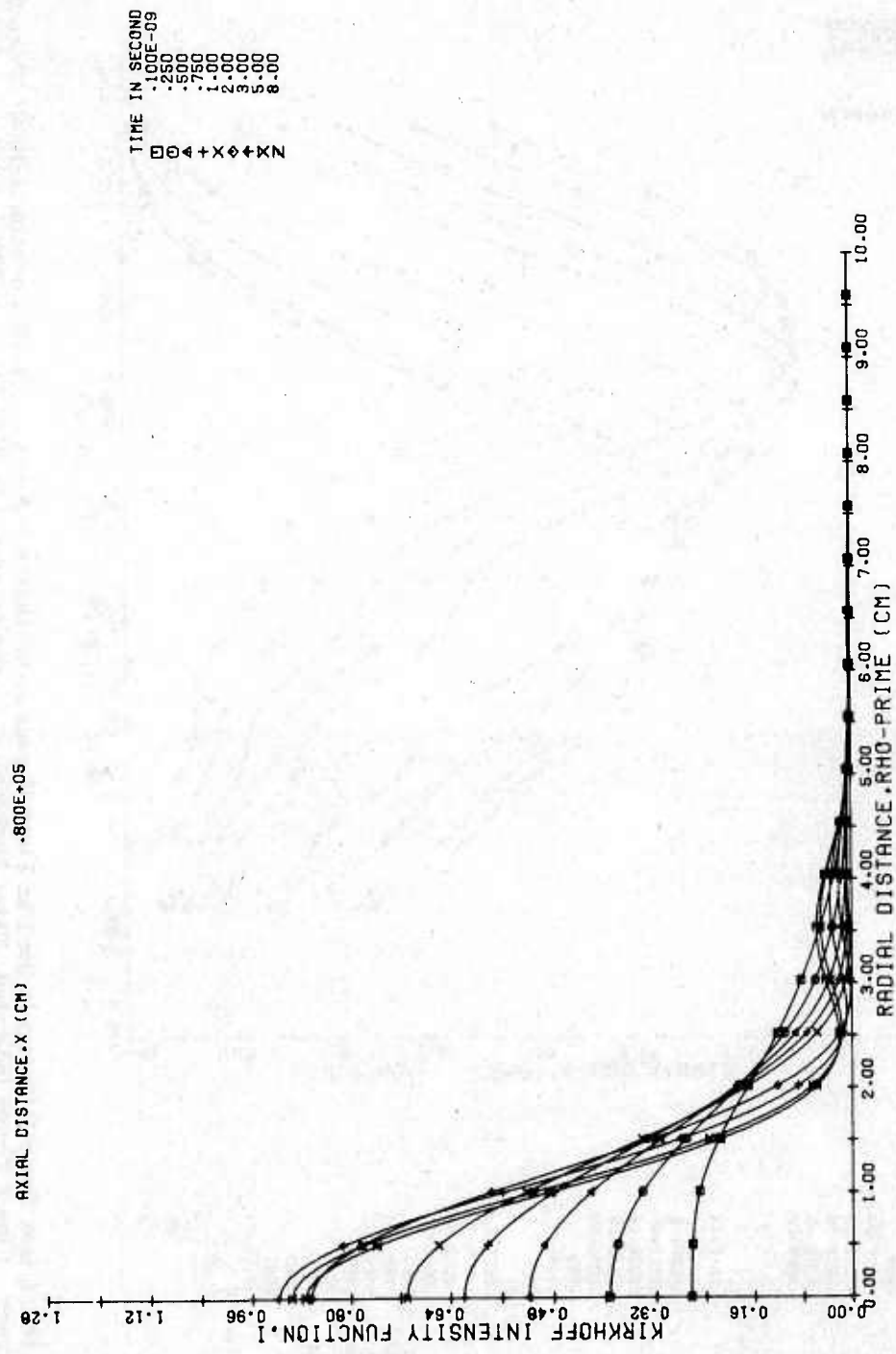


Figure 13. Laser Beam Intensity in the Far Field Versus Radial Distance in a Plane Perpendicular to the Axial Coordinate and at a Distance of 800 m Along the Axis for the 9 Times Indicated. Model No. 1 was used. Plot command is PLOT (1, 1, X, 100, 31, NAS)

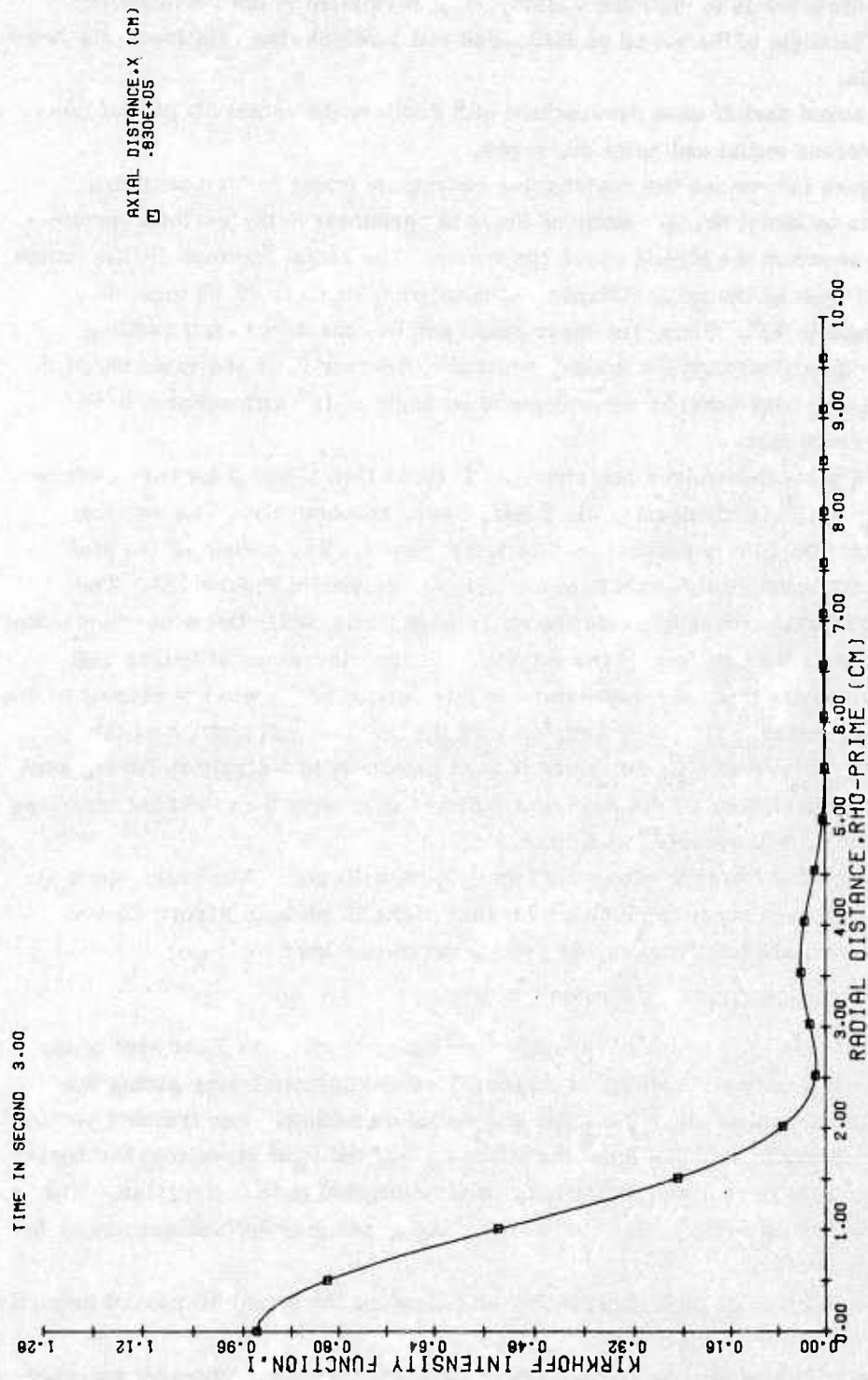


Figure 14. Same as Figure 13, Except That it is in the Gaussian Focal Plane at Time $t = 3$. At this particular instant, this plane is occurring at a distance of 830 m along the axis. Plot command is PLOT (100, 7, X, 100, 34, NA)

which the observer is to view the ensuing 3D plot relative to the rectangular frame. The angle of the arrow is measured counterclockwise relative to the horizontal axis.

The second part of each perspective plot displays the actual 3D plot of temperature versus radial and axial distances.

In Figure 15A we see the rectangular coordinate frame for temperature appropriate to Model No. 1. Some of the data pertaining to the surface normalizations is shown in the legend above the frame. The radial distance (RHO) varies from 0 to 30 cm as the axial distance (Z) runs from -0.65 to +0.65 cm. The viewing angle is 45° . Thus, the laser beam can be considered as travelling vertically upward through the frame, while the observer is on the exit side of the window looking back towards the window at an angle of 45° with respect to the plane of its exit face.

The 3D plots themselves are shown in Figures 15B, C, and D for times corresponding to 10^{-10} (equivalently, 0), 1 and 8 sec, respectively. The vertical height of each 3D plot is proportional to temperature. The corner of the plot closest to the reader corresponds to the arrowed corner in Figure 15A. The narrow horizontal axis represents the outer edge itself, while the wider horizontal axis represents the exit face of the window. As time increases (Figures 15B through D), we see that the temperature in that portion of the window closest to the exit face decreases. This is in keeping with the fact that that portion of the window was initially at 0°C , but since it is in proximity to a highly radiating surface maintained at -100°C , its heat flow outward is greater than the heat input, so its temperature will diminish with time.

A rectangular frame is always drawn with each 3D plot. However, since the rectangular frames corresponding to the rest of the 3D plots in Figure 15 are identical to that shown in Figure 15A, they are omitted here.

6.3.2 PERSPECTIVE INTENSITY PLOTS

Just as in the case of the perspective temperature plot, the first part of the perspective intensity plot exhibits a dimensioned rectangular frame giving the ranges of the distances along the axial and radial directions. The frame's vertical coordinate refers to distance from the window along the axial direction; the horizontal coordinate to radial distance measured orthogonal to this direction. The arrow above the frame indicates the viewing angle, which is defined exactly as in the previous section.

The second part of each perspective plot displays the actual 3D plot of intensity versus radial and axial distances.

In Figure 16A we see the rectangular coordinate frame for intensity appropriate to Model No. 1, together with its appropriate normalizing information. The

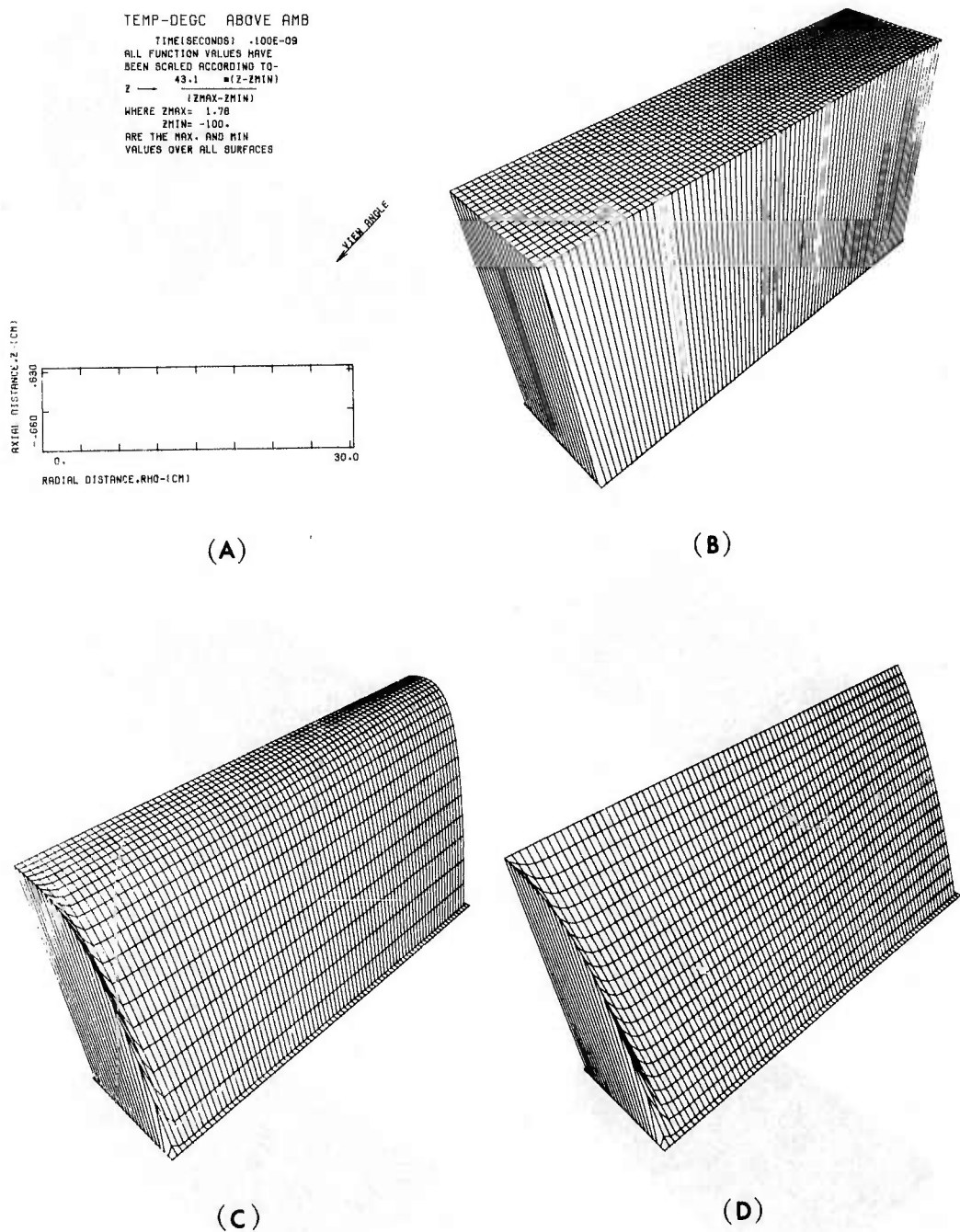


Figure 15. Perspective Temperature Plot for Model No. 1. In (A) are shown the rectangular coordinate frame, indicating the ranges of the radial and axial distances through the window for the ensuing 3D plot, and, the arrow indicating the viewing angle. In (B), (C) and (D) are the 3D plots for times 10^{-10} (that is, 0), 1 and 8 sec, respectively. Plot command is PERSPECTIVE

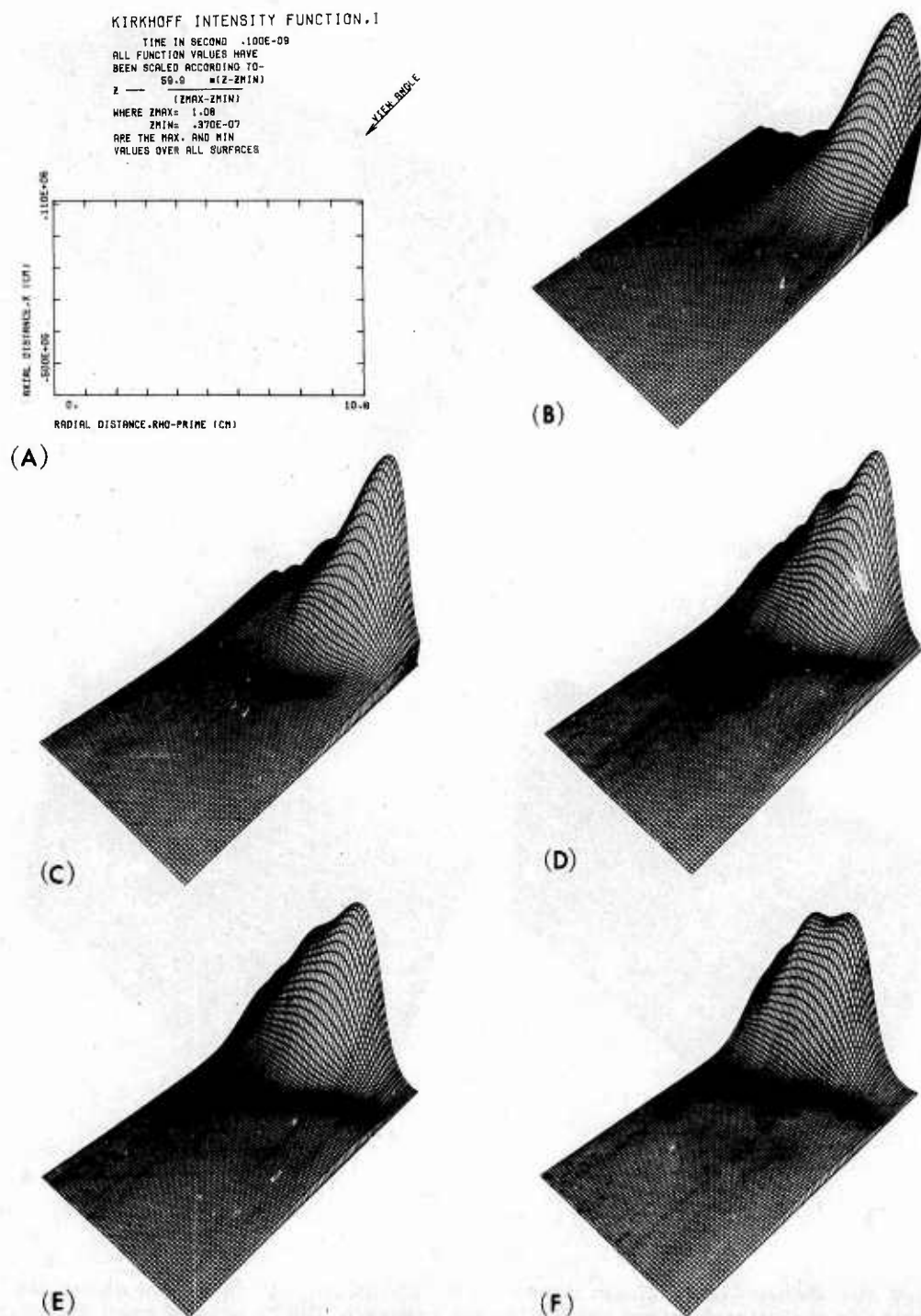


Figure 16. Perspective Intensity Plots for Model No. 1. In (A) are shown the rectangular coordinate frame, indicating the axial and radial ranges in the far field, and, the arrow indicating the viewing angle. In (B), (C), (D), (E) and (F) are the 3D plots for times 10^{-10} (that is, 0, 1, 2, 3 and 8 sec, respectively. Plot command is PERSPECTIVE

axial distance (X) runs from 500 to 1100 m from the window, as the radial distance (RHO-PRIME) varies from 0 to 10 cm. Again, the viewing angle is 45° .

The 3D plots are shown in Figures 16B through 16F, for times corresponding to 10^{-10} (that is, 0), 1, 2, 3, and 8 sec, respectively. The vertical height of each plot is proportional to intensity. The corner of the plot closest to the reader corresponds to the point $X = 1100$ m, RHO-PRIME = 10 cm. The narrow horizontal axis represents the axial distance, while the wider horizontal axis represents the radial distance. As time increases (Figures 16B through 16F), we see the effects of thermal lensing (that is, distortion and defocusing) in the transmitted beam. In the case of ZnSe, the diffraction maximum shifts in towards the window (away from the reader).

The rectangular frames corresponding to the rest of the 3D plots in Figure 16 are also omitted since they are all identical to the one in Figure 16A.

A control is available in the program giving the programmer the option of displaying all of these intensity plots in terms of the normalized coordinates u and v , rather than the dimensioned quantitative X and ρ' .

6.4 Contour Plots

Contour plots are designed to exhibit contours, or "profiles," of constant values of temperature through the window, or of intensity in the far field. The same rectangular frames described in Sections 6.3.1 and 6.3.2 are used and the contours are superimposed upon them.

A set of temperature contours are shown in Figures 17A and B at times of 2 and 8 sec, respectively, for Model No. 1. The symbols designating 20 different temperatures are listed on the left. Since the top horizontal line of the frame represents the exit surface of the window (which is maintained at -100°C), the lower temperatures occur in the upper half of the frame. Figure 17B demonstrates that as time increases, the low temperature contours move toward the entrance face of the window.

We should like to point out that Figures 15D and 17B are displaying temperatures for identical circumstances, that is, the temperature in the window for Model No. 1 after 8 sec. Moreover, the reader should keep in mind that the corner of the perspective plot closest to him in Figure 15D corresponds to the upper right hand corner of the frame in Figure 17B.

Contour plots of 20 intensity values for Model No. 1 at times of 2 and 8 sec are shown in Figures 18A and B, respectively. These two plots can be matched up with the perspective intensity plots of Figures 16D and F, respectively. As above, the corner of the 3D plot closest to the reader corresponds to the upper right hand corner of the rectangular frame. In Figure 18A we see that the diffraction

TEMP-DECC ABOVE AMB

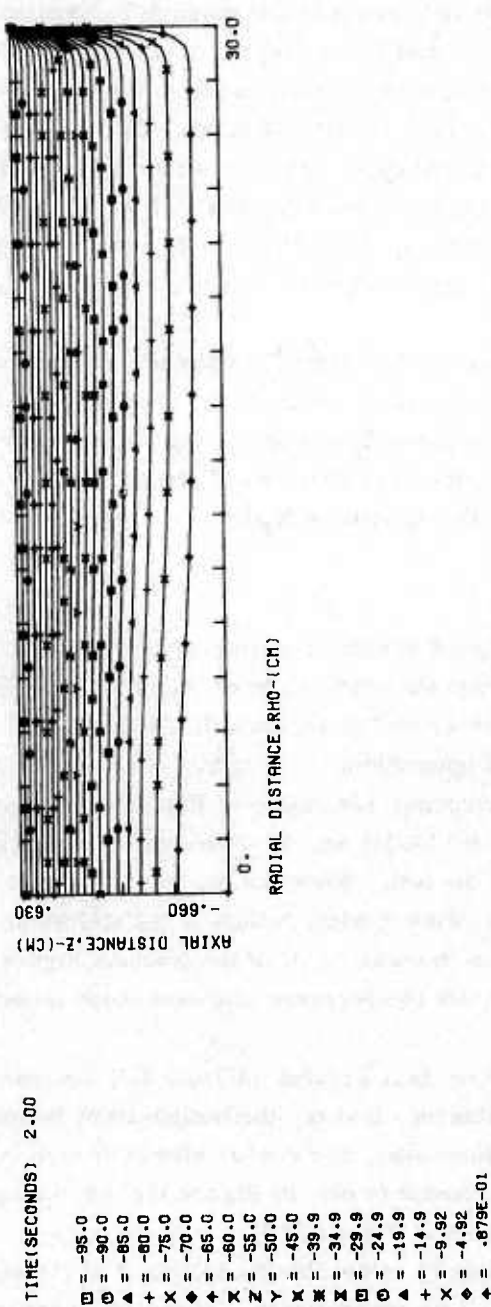


Figure 17A. Contour Temperature Plots for Model No. 1 Showing 20 Temperature Contours at 2 Sec.
Plot command is CONTOUR (3, 6, 20, DN)

TIME(SECONDS) 8.00

□ = -95.2
 ○ = -90.1
 ▲ = -85.1
 + = -80.1
 × = -75.1
 ◆ = -70.1
 * = -65.1
 x = -60.1
 Z = -55.1
 Y = -50.0
 * = -45.0
 x = -40.0
 x = -35.0
 □ = -30.0
 □ = -25.0
 ▲ = -20.0
 + = -15.0
 x = -9.94
 ◆ = -4.93
 * = .816E-01

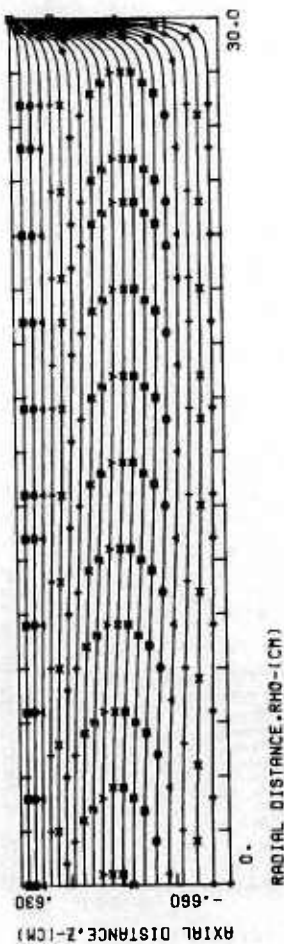


Figure 17B. Contour Temperature Plots for Model No. 1 Showing 20 Temperature Contours at 8 Sec. Plot command is CONTOUR (3, 6, 20, DN)

KIRKHOFF INTENSITY FUNCTION.1

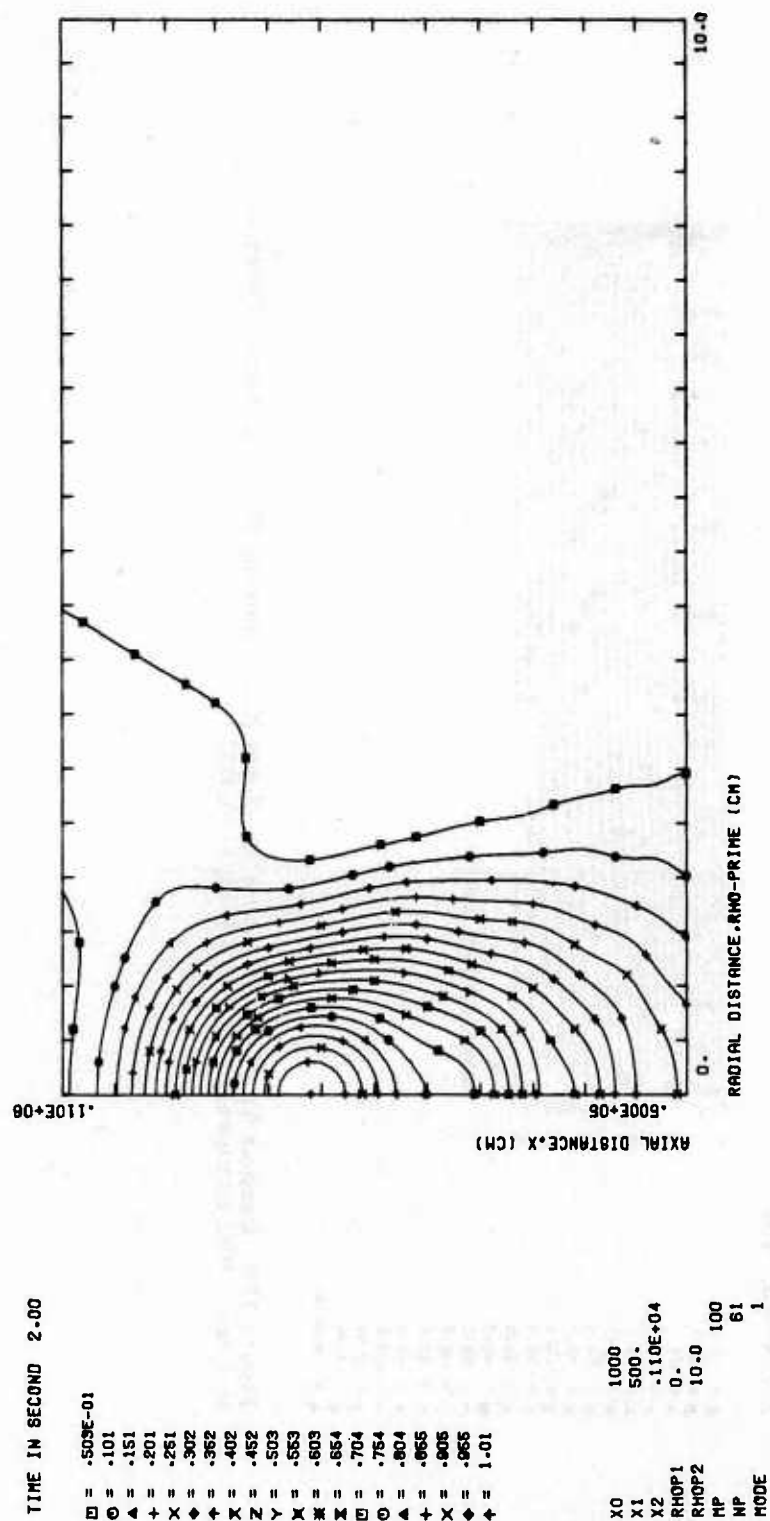


Figure 18A. Contour Intensity Plots for Model No. 1 Showing 20 Intensity Contours at 2 Sec. Plot command is CON-TOUR (3, 6, 20, DN)

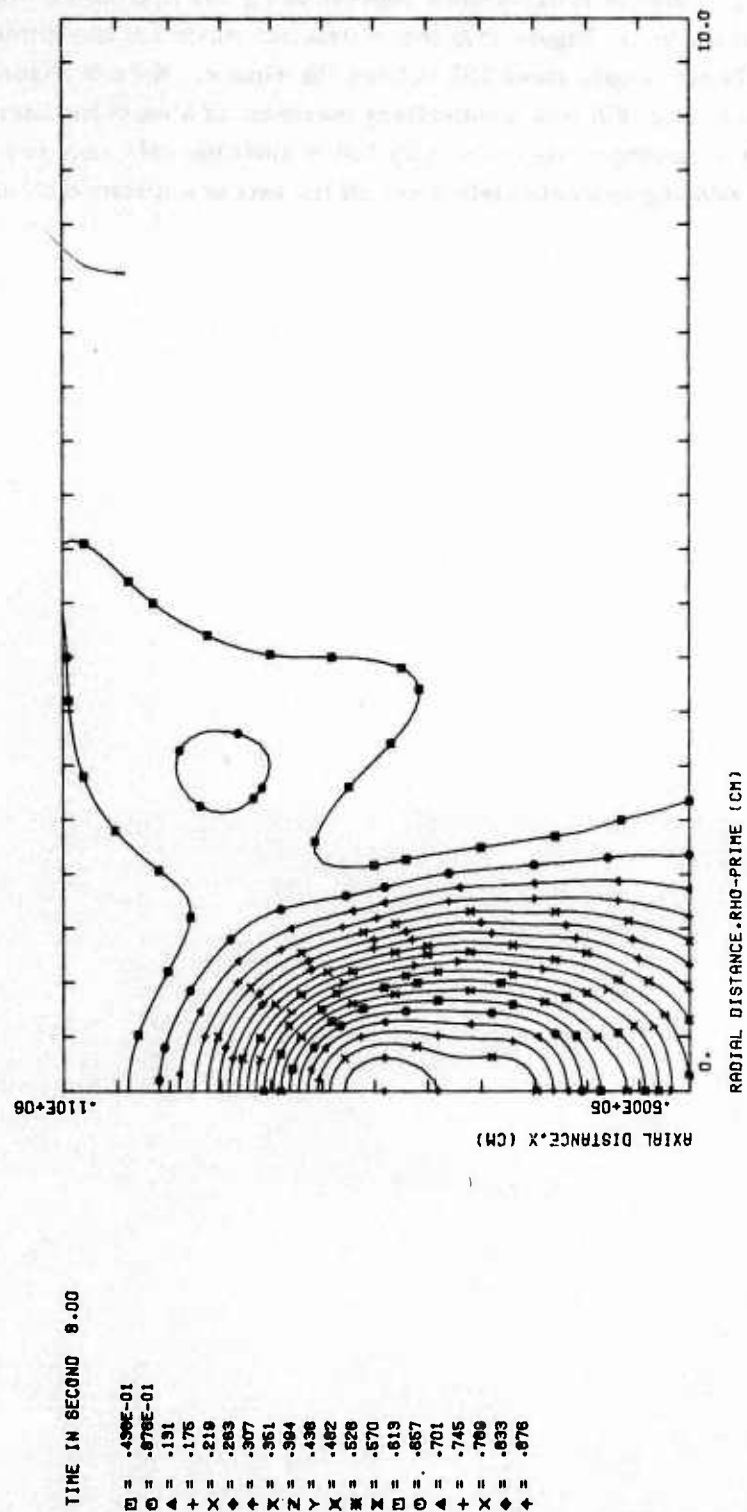


Figure 18B. Contour Intensity Plots for Model No. 1 Showing 20 Intensity Contours at 8 Sec. Plot command is CONTOUR (3, 6, 20, DN)

maximum, having a value of 1.01, occurs approximately 860 m from the window along the axial direction. In Figure 18B, that diffraction maximum has diminished to a value of 0.876 and is only about 790 m from the window. Note in Figure 16F (and somewhat in Figure 18B) how a subsidiary maximum of almost the same intensity value is occurring at approximately 700 m along the axis, and how a minor peak is developing approximately 3 cm off the axis at a distance of about 950 m.

References

VOLUME I

1. Sparks, M. (1971) J. Appl. Phys. 42:5029; and, Jasperse, J.R., and Gianino, P.D. (1972) J. Appl. Phys. 43:1686.
2. Bendow, B., Jasperse, J.R. and Gianino, P.D. (1972) Optics Commun. 5:98.
3. Bendow, B., and Gianino, P.D. (1972) AFCRL-72-0322, unpublished.
4. Bendow, B., and Gianino, P.D. (1973) J. of Electronic Mater. 2:87.
5. Bendow, B., and Gianino, P.D. (1973) Appl. Optics 12:710.
6. Bendow, B., and Gianino, P.D. (1973) Appl. Phys. 2:1.
7. Gianino, P.D., and Bendow, B. (1973) Appl. Phys. 2:71.
8. Weil, R. (1970) J. Appl. Phys. 41:3012; and Bendow, B., Hordvik, A., Lipson, H., and Skolnik, L. (1972) AFCRL-72-0404, unpublished, p. 12.
9. Carslaw, H.S., and Jaeger, J.C. (1959) Conduction of Heat in Solids, 2nd edition, Oxford Press, London (1964) p. 19.
10. Born, M., and Wolf, E. (1964) Principles of Optics, 2nd (revised) edition, Macmillan Co., New York, p. 437.

VOLUME II

11. Carnahan, B., Luther, H.A., and Wilkes, J.O. (1969) Applied Numerical Methods, Wiley and Sons, Inc., New York.
12. Parke, N.G., III (1971) Technical Memorandum No. 4, Parke Mathematical Laboratories, Inc., Carlisle, Massachusetts, unpublished.
13. von Rosenberg, D.U. (1969) Methods for the Numerical Solution of Partial Differential Equations, American-Elsevier Publishing Co., Inc., New York.

14. Ralston, A., and Wilf, H.S. (1967) Mathematical Methods for Digital Computers, Vol. II, Wiley and Sons, Inc., New York.
15. Bendow, B., Gianino, P.D., Hordvik, A., and Skolnik, L.H. (1973) Optics Commun. 7:219; and Skolnik, L.H., Bendow, B., Gianino, P.D., and Cross, E.F. (1974)AFCRL-TR-74-0085 (III), p. 967.
16. Bendow, B., and Gianino, P.D. (1975) Appl. Optics 14:277; and Bendow, B., Gianino, P.D., Flannery, M., and Marburger, J. (1975)Proc. of the Fourth Annual Conf. on Infrared Laser Window Materials, C.R. Andrews and C.L. Strecker (Editors), Advanced Research Project Agcy., Arlington, Virginia, p. 299.